Germline KRAS mutations cause aberrant biochemical and physical properties leading to developmental disorders

Lothar Gremer, Torsten Merbitz-Zahradnik, Radovan Dvorsky, Ion Cristian Cirstea, Christian Peter Kratz, Martin Zenker, Alfred Wittinghofer, Mohammad Reza Ahmadian

Human Mutation

Germline KRAS mutations cause aberrant biochemical and physical properties leading to developmental disorders

Journal:	*Human Mutation*
Manuscript ID:	humu-2010-0192.R2
Wiley - Manuscript type:	Research Article
Date Submitted by the Author:	03-Sep-2010
Complete List of Authors:	Gremer, Lothar; Heinrich Heine University Medical Center, Institute of Biochemistry & Molecular Biology II Merbitz-Zahradnik, Torsten; Heinrich Heine University Medical Center, Institute of Biochemistry & Molecular Biology II Dvorsky, Radovan; Heinrich Heine University Medical Center, Institute of Biochemistry & Molecular Biology II Cirstea, Ion; Heinrich Heine University Medical Center, Institute of Biochemistry & Molecular Biology II Kratz, Christian; DCEG, NCI, Clinical Genetics Branch Zenker, Martin; University Hospital Magdeburg, Institute of Human Genetics Wittinghofer, Alfred; Max-Planck Institute of Molecular Physiology, Department of Structural Biology Ahmadian, Mohammad; Heinrich Heine University Medical Center, Institute of Biochemistry & Molecular Biology II
Key Words:	Noonan syndrome, gain-of-function, GAP resistance, Ras mutations, Ras isoforms

Germline *KRAS* mutations cause aberrant biochemical and physical properties leading to developmental disorders

Lothar Gremer[1#], Torsten Merbitz-Zahradnik[1#], Radovan Dvorsky[1#], Ion C. Cirstea[1#], Christian Peter Kratz[2], Martin Zenker[3], Alfred Wittinghofer[4] and Mohammad Reza Ahmadian[1*]

[1] Institute of Biochemistry and Molecular Biology II, Medical Faculty, Heinrich-Heine University, Universitaetsstr. 1, 40225 Düsseldorf, Germany; [2] Clinical Genetics Branch, DCEG, NCI, 6120 Executive Boulevard, Room EPS 7030, Rockville, MD 20852; [3] Institute of Human Genetics, University Hospital Magdeburg, Leipziger Str. 44, 39120 Magdeburg, Germany; [4] Max-Planck Institute of Molecular Physiology, Department of Structural Biology, Otto-Hahn-Strasse 11, 44227 Dortmund, Germany;

[#] These authors contributed equally to this work.

Running head: Functional impact of *KRAS* germline mutations

[*] Corresponding author: Institute of Biochemistry & Molecular Biology II
Heinrich Heine University Medical Center
Universitätsstr. 1
40225 Düsseldorf
Germany
Phone: #49 211 811 2384
Fax: #49 211 811 2726
E-mail: Reza.Ahmadian@uni-duesseldorf.de

Character count: 36,347

Abstract

The *KRAS* gene is the most common locus for somatic gain-of-function mutations in human cancer. Germline *KRAS* mutations were shown recently to be associated with developmental disorders, including Noonan syndrome (NS), cardio-facio-cutaneous syndrome (CFCS), and Costello syndrome (CS). The molecular basis of this broad phenotypic variability has remained elusive, so far. Here, we comprehensively analyzed the biochemical and structural features of ten germline *KRAS* mutations using physical and cellular biochemistry. According to their distinct biochemical and structural alterations, the mutants can be grouped into five distinct classes that markedly differ from RAS oncoproteins. Investigated functional alterations comprise the enhancement of intrinsic and guanine nucleotide exchange factor (GEF) catalyzed nucleotide exchange, which is alternatively accompanied by an impaired GTPase-activating protein (GAP) stimulated GTP hydrolysis, an overall loss of functional properties, and a deficiency in effector interaction. In conclusion, our data underscore the important role of RAS in the pathogenesis of the group of related disorders including NS (OMIM 163950), CFCS (OMIM 115150), and CS (OMIM 218040) and provide clues to the high phenotypic variability of patients with germline KRAS mutations.

Key words: Noonan syndrome, gain-of-function, GAP resistance, KRAS, Ras isoforms, Ras mutations

Introduction

RAS proteins (HRAS, KRAS 4A, KRAS 4B, and NRAS) are central signal transduction molecules, which act as molecular switches through cycling between an active, GTP-bound and an inactive, GDP-bound state (Vetter & Wittinghofer, 2001). The intrinsic functions of RAS proteins, their GDP/GTP exchange and GTP-hydrolysis, are extremely slow. Guanine nucleotide exchange factors (GEFs) accelerate the exchange of bound GDP for the cellular abundant GTP (Guo et al., 2005), whereas GTPase activating proteins (GAPs) terminate RAS signaling by stimulation of the GTP-hydrolysis reaction (Scheffzek & Ahmadian, 2005). In its GTP-bound form, RAS interacts with and regulates a spectrum of functionally diverse downstream effectors including RAF kinases, phosphatidylinositol 3-kinase (PI3K), and RALGDS (Herrmann, 2003). In the past years, considerable progress has been achieved in understanding the functions and underlying mechanisms of RAS proteins. Comprehensive structural studies resulted in determination of more than 50 structures (Supp. Tables S1 and S2), and provided a deep insight into the three-dimensional fold, the consequences of nucleotide binding and hydrolysis, the principles of regulation by GEFs and GAPs, and the specificity of effector binding (Fiegen et al., 2006). These three classes of interacting proteins predominantly bind to two highly mobile regions, designated as switch I (residues 30-37) and switch II (residues 60-74) (Fig. 1) (Vetter & Wittinghofer, 2001; Sprang, 1997).

Since their discovery as proto-oncogenes 35 years ago, somatic *RAS* mutations have been found to be highly prevalent in a variety of human cancers (Der, 1989; Bos, 1989; Barbacid, 1990; Kranenburg, 2005). The majority of gain-of-function mutations affect amino acid residues G12, G13 and Q61 (Seeburg et al., 1984; Der et al., 1986; Malumbres & Barbacid, 2003) (www.sanger.ac.uk/genetics/CGP/cosmic/) triggering RAS accumulation in the active, GTP-bound state by impairing intrinsic GTPase activity and conferring resistance to GAPs (Ahmadian et al., 1999; Bos et al., 2007; Ahmadian, 2002).

Recently, germline mutations in *HRAS*, *NRAS* and *KRAS* genes have been identified in patients with various developmental disorders including Noonan syndrome (NS), Costello syndrome (CS) and cardio-facio-cutaneous syndrome (CFC) that share several phenotypic abnormalities, such as craniofacial dysmorphism, hair and skin abnormalities, cardiac defects, cognitive impairment, and postnatal growth deficiency (Schubbert et al., 2007a). Moreover, these disorders have reportedly been associated with cancer (e.g., juvenile myelomonocytic leukemia in patients with NS and rhabdomyosarcoma in patients with CS).

HRAS point mutations affecting amino acids at positions 12, 13 and 117 or duplication at position 37 have been associated with CS (Estep et al., 2006; Denayer et al., 2008; Gripp et al., 2006; Sol-Church et al., 2006; Gremer et al., 2010). *NRAS* mutations at positions 50 and 60 have been recently shown to enhance stimulus-dependent MAPK activation and account for rare cases of NS (Cirstea et al., 2010). In contrast, the phenotypic spectrum caused by germline *KRAS* mutations at amino acid positions K5, V14, Q22, P34, I36, T58, G60, V152, D153, and F156 is remarkably broad and comprises NS, CFC and, more rarely, a phenotype consistent with CS (Niihori et al., 2006; Schubbert et al., 2006; Lo, et al., 2009; Kratz et al., 2007; Zenker et al., 2007; Nava et al., 2007; Carta et al., 2006).

The pathophysiological mechanism underlying these clinically related syndromes is most likely a dysregulated signal flow through the RAS/MAPK pathway (Gelb & Tartaglia, 2006; Kratz et al., 2007; Tidyman & Rauen, 2009). To gain insight into the underlying mechanisms, we set out to investigate ten different germline *KRAS* mutants (K5N, V14I, Q22E, Q22R, P34L, P34R, T58I, G60R, D153V, F156L). Results from our global biochemical and functional characterization described in this study provide strong evidence for the existence of distinct structural, mechanistic and functional changes that can result in an overall enhancement of RAS signaling.

Materials and Methods

Plasmids

KRAS cDNA was cloned in pEYFP-c1 vector via *Xho*1 and *Bam*H1. pEYFP-KRAS and ptacHRAS (Tucker et al., 1986) were used as template, respectively, to generate the *KRAS* mutations using a polymerase chain reaction (PCR)-based site-directed mutagenesis protocol as described (Ahmadian et al., 1997). Neurofibromin 1 catalytic domain NF1-333 (amino acids 1198-1531) was cloned in pGEX-4T-1 via *Eco*RI and *Not*1. Gene segments encoding *RAF1-RBD*, *RALGDS-RBD* and *SOS1* catalytic domain CDC25 were cloned in the pGEX vectors as described (Herrmann et al., 1995; Vetter et al., 1999; Lenzen et al., 1998).

Proteins and fluorescent nucleotides

Wild-type and mutant HRAS proteins were prepared from *E. coli* using the ptac-expression system as described (Tucker et al., 1986). The nucleotide-free form of RAS was prepared as described (Ahmadian et al., 2002) and the fluorescent derivatives of GDP, GTP and GppNHp (mantGDP, mantGTP and mantGppNHp) were synthesized according to Ahmadian et al. (Ahmadian et al., 2002). RAS·mantGDP, RAS·mantGTP and RAS·mantGppNHp were prepared as described (Gremer et al., 2008). RAF1-RBD, RALGDS-RBD, the catalytic domains of SOS1 (CDC25) and of neurofibromin (NF1-333) were produced as glutathione S-transferase (GST) fusion proteins in *E. coli*. All proteins were purified as described previously (Ahmadian et al., 2002; Hemsath & Ahmadian, 2005).

Biochemical methods

Various intrinsic and extrinsic biochemical properties of the RAS proteins were measured as described before (Ahmadian et al., 2002; Hemsath & Ahmadian, 2005). The association of mantGDP and mantGppNHp (0.2 µM, respectively) to the nucleotide-free RAS proteins (0.3 µM) was measured in 30 mM Tris pH 7.5, 5 mM $MgCl_2$ and 3 mM DTE at 25 °C using an

Applied-Photophysics stopped flow apparatus. Dissociation of mantGDP from the RAS proteins (0.3 µM) in the presence of 40 µM GDP was measured in 30 mM Tris pH 7.5, 10 mM KP_i, 5 mM $MgCl_2$ and 3 mM dithioerythritol (DTE) at 25°C using a Fluoromax 4 (Horiba Jobin Yvon™) fluorimeter at 366 nm (excitation wavelength) and 450 nm (emission wavelength). Observed rate constants (k_{obs}) of association and dissociation were obtained by single exponential fitting of the data.

GTP hydrolysis of the RAS proteins (1 µM RAS·GTP containing 6 nM $[\gamma]^{32}$GTP) was analyzed in a 30 mM Tris/HCl pH 7.5, 10 mM $MgCl_2$, 3 mM DTE, pH 7.5 buffer at 25 °C by determining the release of radioactive ($^{32}\gamma$)P_i in a charcoal assay. The time courses monitoring the release of radioactive Pi were fitted using single exponential equations. Observed rate constants (k_{obs}) were obtained by single exponential fitting of the data.

GEF-catalyzed mantGDP dissociation from RAS proteins (0.3 µM) was measured in 30 mM Tris/HCl pH 7.5, 10 mM KP_i, 5 mM $MgCl_2$ and 3 mM DTE at 25°C in the presence of CDC25 (2 µM), the catalytic domain of SOS1 and 40 µM GDP using an Applied-Photophysics™ stopped flow apparatus. Observed rate constants (k_{obs}) were obtained by single exponential fitting of the data.

For determination of NF1-333 GAP activity, GDP-bound to RAS mutants was exchanged with excess mantGTP in presence of EDTA to result in a load of higher than 95%. Free unbound nucleotides were removed by gel filtration, and the RAS·mantGTP was immediately snap frozen in liquid nitrogen to avoid unmonitored hydrolysis (Gremer et al., 2008). GAP-stimulated GTPase reaction of RAS proteins (0.2 µM) was measured in 30 mM Tris pH 7.5, 10 mM $MgCl_2$ and 3 mM DTE at 25 °C using a Hightech™ stopped-flow apparatus. The monitored reactions show an increase of fluorescence due to association of NF1-333 (2 µM), the catalytic domain of neurofibromin 1, with RAS·mantGTP, and a subsequent hydrolysis of mantGTP, described by a decrease of fluorescence. This decrease, we fitted by a single exponential.

Effector binding assay was performed in 30 mM Tris/HCl pH 7.5, 100 mM NaCl, 5 mM $MgCl_2$ and 3 mM DTE at 25 °C using a Fluoromax 4 fluorimeter in polarization mode. Increasing amounts of GST-tagged RAS binding domains (RBD) of RAS effectors were titrated to 0.3 µM mantGppNHp-bound RAS proteins resulting in an increase of polarization. The concentration dependent binding curve was fitted using a quadratic ligand binding equation.

Cell-based assays

Monkey kidney epithelial COS-7 cells were grown in DMEM supplemented with 10 % fetal calf serum (FCS) and transiently transfected using DEAE-dextran as described (Herbrand & Ahmadian, 2006).

GST pull down and MEK1/2, ERK1/2, and AKT activation assays were performed as described (Cirstea et al., 2010). Briefly, the levels of GTP-bound RAS were determined using GST-fused RAF1-RBD protein to pull down active GTP-bound RAS by glutathione beads from extracts of COS-7 cells transfected with the respective KRAS mutants. The beads were washed four times and subjected to SDS-PAGE (15 % polyacrylamide). Bound RAS proteins were detected by Western blotting using monoclonal antibodies against RAS (anti-RAS antibody, BD Transduction Laboratories™), anti-RAS (clone RAS10, Upstate-Millipore™). MEK1/2, ERK1/2, AKT, phospho-MEK1/2, phospho-ERK1/2 and phospho-AKT, respectively, were determined by Western blotting analysis of the same COS-7 cell lysates used for the RAS pull down assay and were detected using antibodies against MEK1/2 (Cell Signaling™), ERK1/2 (Cell Signaling), AKT (Cell Signaling), phospho-MEK1/2 (Ser 217/221, Cell Signaling), phosphor-ERK1/2 (Thr202/Tyr204, Cell Signaling), phospho-AKT (Ser473, Cell Signaling).

Structural analysis

Because no $KRAS^{wt}$ structure is available to date, the structures of HRAS were used in our study. The G-domains of HRAS and KRAS share 97% identity and are generally accepted to be very similar in structure and function (Ahmadian et al., 1997). The differences between the active and inactive state of RAS were analyzed by comparison of the GDP-bound (Milburn et al., 1990) [Protein Data Bank (PDB) code 4Q21] and GTP-bound (Pai et al., 1990) [1CTQ] HRAS structure, respectively. These structures were selected because they represent wild-type RAS (RAS^{wt}) protein and have high resolutions among GDP- or GTP-bound structures. The interactions of RAS with its binding partners were analyzed on the basis of HRAS structure in complexes with $p120^{RASGAP}$ (Scheffzek et al., 1997) [1WQ1], the GEF SOS1 (Margarit et al., 2003) [1NVV], and the downstream effectors, RAF1-RBD (Nassar et al., 1995) [1C1Y], PI3Kγ (Pacold et al., 2000) [1HE8], BYR2-RBD (Scheffzek et al., 2001) [1K8R], RALGDS (Huang et al., 1998) [1LFD] and PLCε (Bunney et al., 2006) [2C5L].

Results

Since HRAS and KRAS proteins share 97 % amino acid sequence identity in their G-domain and are 100% identical in regions responsible for interactions, their structural and biochemical properties can be considered to be very similar (e.g. D153 in KRAS is E153 in HRAS) if not identical (Ahmadian et al., 1997). Furthermore, for a comprehensive structure-function analysis, no wild-type KRAS structure is available to date. Thus, respective KRAS mutations were analyzed using HRAS structures (Supp. Tables S1 to S3), and for practical reasons we generated these *KRAS* mutations (K5N, V14I, Q22R/Q22E, P34R/P34L, T58I, G60R, E153V, and F156L; Fig. 1A) in the context of both the *HRAS* gene in the *Escherichia coli* expression system and the KRAS gene in the eukaryotic expression system. Purified mutant RAS proteins were comprehensively characterized using advanced physical and cellular biochemistry. As controls, we used wild type RAS (RAS^{wt}), a GTPase deficient mutant

(RAS^{G12V}) and a self-activating ("fast-cycling") mutant (RAS^{F28L}) (Reinstein et al., 1991). All data are summarized in Tables 1 and Supp. Table S4.

Germline RAS mutations are located at permissible structural sites

Overall location and spatial orientation of the mutated amino acids according to the nucleotide-bound forms were deduced from the structures of HRAS in the inactive, GDP-bound state (Fig. 1B) and in the active, GTP-bound state (Fig. 1C), respectively. We inspected solvent accessible areas of considered residues (Supp. Table S3) and found that only T58 and G60 undergo significant conformational rearrangements between the active and inactive state. These differences are not unexpected as these residues are nearby or part of the switch II region (Fig. 1). An interesting exception is P34, which is almost equally solvent exposed in both states although it is part of switch I (Figs. 1B and 1C; Supp. Table S3). The absolute solvent accessible area of P34 is relatively large in contrast to T58 and G60 (Figs. 1B and 1C; Supp. Table S3).

To assess if the mutations directly interfere with intermolecular interactions, we analyzed structures of RAS in complexes with regulators and effectors (Supp. Table S2). Remarkably, only P34 is clearly located within the interacting interface contacting GAPs, GEFs and effectors (Supp. Fig. S1, yellow areas; Supp. Table S3). Other investigated residues are either on its edge or buried within the protein and are thus not directly participating in the interaction with RAS binding partners (Supp. Fig. S1; Supp. Table S3). Interacting interfaces (Supp. Fig. S1, yellow areas) are rather distinct between the complexes with SOS1 as compared with GAP and effectors. Among the RAS mutants, three residues, P34, T58 and G60, contact the CDC25 domain of SOS1 (Supp. Table S3). As mentioned above, G60 is solvent exposed in the GDP-bound state (Fig. 1B; Supp. Table S3), which should be also true for an arginine side chain in the case of RAS^{G60R} (Supp. Fig. S1A). In this scenario a large, positively charged side chain would interfere sterically with the CDC25 binding.

Alternatively, it is also possible that an arginine within the highly conserved DxxG^{60}QE motif (part of the switch II, Fig. 1A), may interfere with the nucleotide dissociation itself. This motif has been recently implicated to play a critical role in GEF-mediated nucleotide exchange reactions (Gasper et al., 2008).

Finally, we calculated the vicinity of investigated amino acid residues to the nucleotides (Supp. Table S3) to explore a possible direct impact of the various mutations on GDP/GTP binding and GTP hydrolysis, respectively. Only two residues, V14 and G60, are involved in direct interaction with the nucleotide. Since V14 contacts the nucleotide with backbone atoms, only the substitution of G60 can directly affect nucleotide binding and hydrolysis as its Cα atoms faces the γ-phosphate in the GTP state.

Germline RAS mutants accumulate in the GTP-bound state

To gain insights into the regulatory cycle of the RAS mutants in cells we transiently transfected COS-7 cells with plasmids expressing KRAS^{wt} and KRAS mutant proteins. We determined the amount of active, GTP-bound RAS in the presence of serum using GST-fusion proteins of the RAS-binding domain (RBD) of RAF1 (GST-RAF1-RBD) immobilized on glutathione sepharose (GST pull down assay described in Materials and Methods section). Figure 2A shows that the majority of the RAS mutants exhibit a tremendously high level of activation as compared to RAS^{wt}. We next repeated these experiments under serum starved conditions in order to exclude RAS activation by serum-containing stimuli. The majority of the RAS mutants remarkably remained in a hyperactive state except for K5N, Q22R and D153V (Fig. 2B, upper panel). Two major reasons for the high level of GTP-bound active RAS mutants have to be considered: an increased GDP/GTP exchange (“fast cycling”) or a reduction of intrinsic or/and GAP-stimulated GTP hydrolysis.

It is important to note that point mutations may lead to changes in RAS (epitope) recognition by the antibody. Therefore, we repeated these experiments using two different anti-RAS

antibodies (Fig. 2 and Supp. Fig. S2), and found that the P34L and P34R mutants are not recognized by anti-RAS antibody clone RAS10 from Upstate-Millipore™, but can be detected with the antibody anti-RAS obtained from BD Transduction Laboratories™, and that the mutant D153V is much better recognized by the BD Transduction Laboratories™ anti-RAS (Figs. 2 and Supp. Fig. S2). These observations indicate that the affinity of antibodies towards tested protein can be impaired by point mutation.

Increase in nucleotide exchange of RAS^{V14I}, RAS^{Q22E} and RAS^{F156L}

To examine the GDP/GTP exchange of the mutants, we measured both intrinsic and GEF-catalyzed nucleotide dissociation (Fig. 3). The most significant effect was an increase in dissociation of the fluorescently labeled GDP (mantGDP) from RAS mutants by almost 30-fold in the case of V14I and Q22E, and more than 60-fold in F156L (Fig. 3B). The fact that these mutants release mantGDP even faster than the already established "fast cycling" F28L mutant (Reinstein et al., 1991) leads, most likely, to a GEF-independent activation of these mutants in cells (Fig. 2). For completeness, we also measured the intrinsic functions of the RAS mutants concerning nucleotide association (Supp. Fig. S3). Interestingly and in contrast to the oncogenic G12V mutant and the "fast cycling" F28L mutant, the association rates of mantGDP or a non-hydrolyzable fluorescently labeled GTP analog (mantGppNHp) with all other RAS mutants are slower then that of wild type reaching a maximum 20-fold difference in the case of K5N (Supp. Fig. S3). However, as with RAS^{wt}, no preference for a particular nucleotide was observed, and thus, the difference in association kinetics would probably have no major functional consequence due to the high affinity of guanine nucleotides to RAS and due to their high concentration in the cell.

The dissociation of mantGDP from RAS^{wt} catalyzed by the catalytic domain of SOS1 (CDC25) (Pechlivanis et al., 2007) is three orders of magnitude faster than in the absence of this GEF (Fig. 3) under the conditions used. The effect of the germline RAS mutations on the

CDC25-mediated dissociation was measured under the same conditions. Interestingly, differences in GEF-catalyzed nucleotide exchange reactions (Figs. 3C and D) correlate with the intrinsic dissociations of mantGDP from RAS proteins (Figs. 3A and B). This suggests that the observed differences in the acceleration of nucleotide exchange between wild type and mutant RAS are caused primarily by structural changes of RAS itself, and not by altered RAS-GEF interactions. An exception is RAS^{G60R} that was virtually unresponsive towards CDC25 under our experimental condition, which is most likely due to the lack of a RAS-CDC25 interaction. Besides G60, the residues P34 and T58 also contact the CDC25 domain of SOS1 (Supp. Table S3), but obviously only the substitution of G60 to arginine abolishes the formation of the Ras-CDC25 complex, as no acceleration of nucleotide exchange by SOS1 was observed for the G60R mutant (Figs. 3C and D).

Profound GAP insensitivity of the RAS^{P34} and RAS^{G60} mutants

Mutants that do not exhibit a fast nucleotide exchange but accumulate in an active, GTP-bound form are strongly suggestive of having an impaired GTP hydrolysis activity. Therefore, we investigated the GAP sensitivity of the RAS mutants in cells. For this purpose, the catalytic domain of neurofibromin (NF1-333) (Ahmadian et al., 1997) was added to the cell lysates before performing the GST pull down assay. The middle panel of Figure 2B shows that RAS^{P34L}, RAS^{P34R} and RAS^{G60R} are GAP resistant and locked in the active state in a fashion similar to oncogenic RAS^{G12V}. Conversely, these results indicate that GAP-sensitive mutants RAS^{V14I}, RAS^{Q22E}, RAS^{T58I} and RAS^{F156L} most likely have an increased GDP/GTP exchange explaining their accumulation in the active state (Fig. 2B, upper panel).

Next we examined the capabilities of RAS mutants to hydrolyze GTP in the absence and in the presence of a RAS-GAP *in vitro*. Intrinsic GTP hydrolysis was drastically reduced by the substitution of G60 by arginine, even more than the decrease caused by the oncogenic mutation G12V (Figs. 4A and B). All other RAS mutations altered the intrinsic GTP

hydrolysis only marginally. A different situation was obtained for the GAP-stimulated GTPase activity after adding the catalytic domain of neurofibromin 1 (NF1-333). Six of ten RAS mutants, Q22E, Q22R, P34L, P34R, G60R, and F156L revealed considerable reduction in GAP-stimulated GTPase rates (Fig. 4D) compared to Ras^{wt}. Among them, Q22E and F156L also showed faster intrinsic and GEF-catalyzed nucleotide dissociation as described above (Figs. 3B and D). The most severe impairment of the GAP-stimulated GTP hydrolysis is caused by the mutations P34L, P34R and G60R which is comparable to that of the oncogenic mutation G12V. Earlier mutational studies of RAS also showed that substitution of P34 by arginine abolished the GAP-stimulated GTP hydrolysis reaction (Stone et al., 1993; Chung et al., 1993). The other RAS mutants, K5N, V14I, T58I and E153V exhibited similar k_{obs} values of stimulated GTP hydrolysis as obtained for RAS^{wt} (Fig. 4D). However, a recent report discussed that RAS^{V14I} exhibits a much lower GTP-hydrolysis in the presence of RAS-specific GAPs (Schubbert et al., 2006). This discrepancy is possibly due to the different method used for the investigation of the GAP sensitivity. In contrast to our study, the former report used GST-fusion proteins of the respective RAS mutants and GAP proteins. In addition, unlike the nitrocellulose filter binding assay used by Schubbert et al. (Schubbert et al., 2006), our studies are based on time-resolved fluorescence measurements using single turnover stopped-flow techniques in solution.

Moderate gain of signal transduction through the germline RAS mutants

Accumulation of the KRAS mutants in their active state as a consequence of increased nucleotide exchange and impaired interaction with GAPs would predict a sustained activation of effectors and cellular signal transduction. To examine whether the elevated GTP-bound state of these proteins is correlated with an increased downstream signaling, we measured levels of phosphorylated MEK1/2, ERK 1/2 and AKT in COS-7 cells transiently transfected with the KRAS mutants. To avoid any upstream propagation by extracellular stimuli seen in

experiments performed in the presence of serum (Fig. S4), we analyzed the potential of the germline KRAS mutants themselves to activate signaling pathways under serum-free culture conditions (Fig. 5). Given the abnormal biochemical properties that resulted in massive accumulation in the GTP-bound, active forms as shown above (Fig. 2B, upper panel), a strongly increased downstream signaling was expected. Surprisingly, most germline KRAS mutants induced only moderately increased phosphorylation levels of downstream signaling proteins. $KRAS^{V14I}$, $KRAS^{Q22E}$ and particularly $KRAS^{F156L}$ but also perceivably $KRAS^{P34R}$ and $KRAS^{G60R}$ showed increased levels of phosphorylated MEK1/2 (pMEK1/2), ERK1/2 (pERK1/2) and AKT (pAKT) as compared to RAS^{wt} but less than RAS^{G12V} (Fig. 5). These results emphasize the ability of the majority of the germline KRAS mutants to activate downstream effectors under serum-free conditions to moderate degree. Expression of the KRAS mutants in presence of serum (Supp. Fig. S4) leads to overall enhanced MEK1/2 phosphorylation (e.g. K5N, V14I, Q22E, T58I, D153V, F156L) and enhanced ERK1/2 phosphorylation (e.g. V14I, Q22E, Q22R, F156L). These findings suggest that increased downstream signaling is a consistent feature of germline KRAS mutations, but this effect remains stimulus-dependent in some mutants, while it is constitutive in others.

Significant loss of effector binding affinity

Our data show that most KRAS mutants accumulate in the active, GTP-bound form to an extent that can be similar to oncogenic RAS^{G12V}, but are disabled to equally activate downstream pathways, suggesting that an interaction with the downstream effectors might be impaired. Therefore, we set out to explore the impact of the investigated patient mutations on the interactions with the RAS-binding domains of two well-studied effectors RAF1 kinase and RALGDS. For this purpose, we established a fluorescence polarization-based assay (see Materials and Methods section), which enabled us to determine the equilibrium dissociation constants (K_d) of RAS·effector complexes (Fig. 6 and Supp. Fig. S5).

Downstream effectors bind with a much higher affinity to the GTP-bound form of RAS than to its GDP-bound form (Herrmann et al., 1995). We quantified binding constants by fluorescence polarization for the interaction of RAS with the RAS-binding domain (RBD) of RAF1 (RAF1-RBD) (Fig. 6B) or with the RBD of RALGDS (RALGDS-RBD) (Supp. Fig. S5). Since RAS effectors, including RAF1, RALGDS and PI3K share an overlapping interactive region on GTP-bound RAS with GAPs (Supp. Figs. S1B, S1C and S1D) (Vetter & Wittinghofer, 2001), it is not surprising that most RAS mutations, which interfered with the GAP activity (Fig. 4D), also interfered with RAF1 and RALGDS binding (Fig. 6 and Supp. Fig. S5). The strongest reduction in binding affinity is observed with RAS mutations at position P34, G60 and F156. Taken together, our studies show that the remarkable increase in RAS activation (Fig. 2B, upper panel) due to GAP resistance or reduction of GAP interaction (Figs. 4D and 2B, middle panel), which is most prominent in the case of P34 and G60 mutations, is at least in part compensated by another functional impairment, namely the significant loss of interaction with downstream effectors of up to 125-fold (K_d value of 27.6 µM for $KRAS^{P34L}$ divided by 0.22 µM for $KRAS^{wt}$) (Fig. 6B).

Discussion

For over three decades the biochemical effects exhibited by cancer-associated RAS mutations have been studied in great detail. In contrast, only limited information is available on the newly discovered germline mutations of RAS. The data presented herein represent the most comprehensive biochemical and structural analysis of these novel RAS mutants to date.

The key phenomenon in RAS biology is its nucleotide-dependent interaction with different proteins of the signal transduction machinery, which is controlled by the GDP/GTP exchange and the GTP hydrolysis reactions. Any change of these functions or an impairment of the interaction of RAS with its binding partners can affect the fine-tuned balance of RAS

regulation and its activity in cells. It is now clear that aberrant RAS function in the developing embryo leads to an abnormal progression of developmental programs. Understanding the mechanisms by which aberrant RAS disturbs normal development represents an important scientific goal. The results of this study confirm the notion that germline *KRAS* mutations generally confer a milder gain-of-function phenotype than cancer-associated mutations at positions G12, G13 or Q61. Moreover, we show that germline *KRAS* mutations caused multifaceted effects which cannot simply be explained to result from one of the underlying mechanisms fine-tuning RAS functions. To gain insights into the structural alterations caused by the germline *KRAS* mutations, we inspected the environment of the respective residue and compared them with RAS^{wt} to explain their functional properties (Supp. Fig. S7, and "*Assessement of possible structural consequences of RAS mutants*" in electronic supporting information). As summarized below and in Table 1 and Supp. Table S4, our data strongly suggest the existence of five partially interrelated mechanistic classes of KRAS mutants with altered signal transduction:

Class A groups the mutants $KRAS^{K5N}$, $KRAS^{T58I}$ and $KRAS^{D153V}$, which do not show major biochemical alterations compared to wild-type KRAS *in vitro*. All three mutants, especially T58I, are in a higher activated state and show a higher downstream signaling as compared to RAS^{wt} indicating that mutation at these positions do impact RAS function but could not be monitored by the current tools of RAS biochemistry. $KRAS^{D153V}$ expressing cells showed a slightly higher GTP-bound level and an increase in MEK phosphorylation as compared to $KRAS^{wt}$ but no difference regarding pERK and pAKT levels. The reason for this observation is not fully understood yet.

On the other hand, we have recently shown in a similar situation with $NRAS^{T50I}$ identified in NS patients, that the residue T50 does not play a functional role, neither in nucleotide binding and hydrolysis nor in contacting protein partners of NRAS but rather in the interaction with membrane lipids (Cirstea et al., 2010). By inspecting such a RAS/membrane model (Abankwa

et al., 2008), it is rather tempting to speculate that the E153 (in HRAS)/D153 (in KRAS) side chain may directly influence RAS interaction with the membrane. Moreover, we superposed HRAS with a recently published KRAS mutant structure (Supp. Table S1), which clearly showed that there is no significant difference between the E153 and D153 positions (Supp. Fig. S6).

Class B represented by KRAS^{V14I}, showed a dramatic increase, both in intrinsic and GEF-catalyzed nucleotide exchange as the probable major cause for its accumulation in the GTP-bound state and increased downstream signaling. In contrast to a previous study, where KRAS^{V14I} exhibited a significantly lower GTP-hydrolysis in the presence of RAS-specific GAPs *in vitro* (Schubbert et al., 2006), we did not observe any changes in the intrinsic and GAP-stimulated GTP-hydrolysis reactions (Fig. 4) and an only mild decrease in effector binding affinity.

Class C is represented by KRAS^{Q22R}, and characterized by an impaired GAP-stimulated GTP hydrolysis while its intrinsic functions including the intrinsic GTP hydrolysis reaction (Fig. 4) remained unaffected and its interaction with effectors is virtually functional (Fig 6). Consistent with our results, a KRAS^{Q22K} mutant, which is physiologically homologous to Q22R, has been shown to transform NIH-3T3 fibroblasts (Tsukuda et al., 2000), an effect that is presumably caused by accumulation of RAS in its GTP-bound, active state. The underlying pathogenetic mechanism is most likely due to a surface exposed guanidinium group of the arginine which prevents GAP binding (Supp. Fig. S7C) but does not interfere with effector binding (Fig. 6).

Class D comprises the mutants KRAS^{Q22E} and KRAS^{F156L}. The members of this class are characterized by an increase in intrinsic and catalyzed nucleotide exchange in combination with the resistance to GAPs, but still with a functional interaction with effectors. These effects which cause a profound activation of the MAPK and PI3K/AKT pathways are not directly affecting nucleotide binding and hydrolysis (Figs. 3 and 4) since Q22 and F156 are not

directly involved in the coordination of the active center. F156 substitution by leucine creates a cavity within the hydrophobic core causing loss of contact with surrounding residues (Supp. Fig. S7E), which lead to an overall reduction of the nucleotide binding affinity (Xu et al., 1998), an increase in the cellular level of GTP-bound RAS and subsequent activation of the transforming potential of RAS (Quilliam et al., 1995).

All mutations that cause faster dissociation ($KRAS^{V14I}$, $KRAS^{Q22E}$, $KRAS^{F156L}$) in comparison to RAS^{wt} affect amino acids that are either barely (V14, Q22) or not at all (F156) exposed on the RAS protein (Figs. 1B and C; Supp. Table S3). It implicates that disturbed integrity of RAS structure is responsible for the alteration of this intrinsic property as the substitutions of buried amino-acids by smaller side-chains very likely affect the internal dynamics of the proteins.

Class E is represented by the mutants $KRAS^{P34L}$, $KRAS^{P34R}$ and $KRAS^{G60R}$ and is characterized by a defective GAP sensitivity and a strongly reduced interaction with effectors. Although these mutants are locked in a hyperactivated state, which is rather comparable to the oncogenic RAS^{G12V}, their ineffectiveness for downstream signaling in turn causes only a mild gain-of-function phenotype. Accordingly, class E mutants are able to activate downstream pathways as shown by ERK and AKT phosphorylation (Fig. 5). A similar case has been recently reported in a germline HRAS mutant associated with CS (Gremer et al., 2010). Hereby, E37 duplication in the switch I region of HRAS impairs both binding of GAP and effector proteins. Therefore, this mutant can also be assigned as a class E member. Although $KRAS^{P34L}$ and $KRAS^{P34R}$ do not respond to GAP they are in principle able to hydrolyze GTP intrinsically (Fig. 4). This strongly suggests that the respective amino acid substitutions either interfere with GAP binding or with the positioning of the catalytic arginine of GAP in the active site. P34 is invariant in RAS and RHO proteins (Eberth et al., 2005) and any substitution of P34 has been suggested to affect interaction with the binding partner of RAS (Chung et al., 1993; Stone et al., 1993).

The mutation of KRAS G60 to arginine has most severe consequences, namely an overall impairment of almost all biochemical and functional properties. Its substitution by a large and charged amino acid like arginine in KRAS or glutamate in NRAS (Cirstea et al., 2010) seems to corrupt the switch regions including the critical catalytic Q61, affect nucleotide binding, GTP hydrolysis and impairs intermolecular interaction with regulators and effectors. Previous studies have shown that a conservative mutation of G60 to alanine impairs the normal GTPase function of RAS and Gα (Sung et al., 1996; Ford et al., 2005). G60A mutation of HRAS dramatically affects intrinsic and GAP-stimulated GTP hydrolysis without major changes on its interaction with effector proteins (Hwang et al., 1996). Structural analysis of $HRAS^{G60A}$ showed that its switch I region adopts an open conformation (Ford et al., 2005). However, G60 substitution by arginine (KRAS) or glutamate (NRAS) may affect both switch regions, which in turn may be the reason for loss of intrinsic and extrinsic functions.

Interestingly, certain RAS mutations such as P34L, P34R or G60R are compromised in their interaction with effectors as evidenced by the inability to bind efficiently RAF-RBD or RALGDS-RBD (Fig. 6 and Supp. Fig. S5). This is surprising considering that enhanced downstream signaling is the primary cause of the developmental diseases. At the same time, these mutations have the most severe effect on the GAP-mediated GTPase reaction, in a range that is quite similar to the oncogenic mutation prototype G12V. It is likely that the impairment of effector interactions damps the consequences of GAP resistance of these mutants on downstream signal flow. This is in contrast to RAS proteins with oncogenic mutations at the positions G12 or Q61, which show a comparably tight interaction with effectors as RAS^{wt} (Gremer et al., 2008). Our results therefore provide an explanation for the lower levels of activated KRAS signaling exerted by germline mutations compared to the classical oncogenic mutations. The fact that the majority of investigated amino acids of RAS are neither involved in contacts with interacting partners nor with the nucleotide also suggests that the effects of changes at these sites are milder compared to oncogenic mutations and may at least in part

explain why these alterations are tolerated in the germline and are generally not associated with tumor development in affected individuals.

The diversity of functional consequences of germline *KRAS* mutations is paralleled by a remarkably wide phenotypic spectrum associated with mutations in this gene and its tempting to assume a causal relation between certain genotypes and phenotypic expressions. There is indeed a tendency towards an association of more severe phenotypes (CFC/CS) with mutations that proved to have stronger effects on ERK phosphorylation in our experiments (Q22E, Q22R, P34R, G60R, F156L) (Fig. 5). In contrast, patients harboring the mutations V14I, P34L, D153V tend to have less severe physical and mental handicaps and are more commonly classified as having NS, the less severe form among this group of developmental disorders (Aoki et al., 2008). However, the number of known patients with a proven *KRAS* mutation is still too small to delineate clear genotype - phenotype correlations.

In conclusion, we describe and classify in detail the functional properties of a spectrum of germline mutations of *KRAS* that have been previously identified as a cause of developmental syndromes. Our studies reveal several new mechanisms by which germline *KRAS* mutations contribute to human disease and lead to disturbed embryonic development.

Acknowledgements

We thank Dorothee Vogt and Patricia Stege for expert technical assistance and Katja T. Koessmeier for critical reading of the manuscript. The study was supported in part by grants of the German Research Foundation (DFG AH 92/5-1), the NGFNplus program of the German Ministry of Science and Education (BMBF, grant 01GS08100) and the Research Committee of the Medical Faculty of the Heinrich-Heine University Düsseldorf.

References

Abankwa D, Hanzal-Bayer M, Ariotti N, Plowman SJ, Gorfe AA, Parton RG, McCammon JA, Hancock JF. 2008. A novel switch region regulates H-ras membrane orientation and signal output. *EMBO J.* **27**: 727-735.

Ahmadian MR. 2002. Prospects for anti-ras drugs. *Br. J Haematol.* **116**: 511-518.

Ahmadian MR, Hoffmann U, Goody RS, Wittinghofer A. 1997. Individual rate constants for the interaction of Ras proteins with GTPase-activating proteins determined by fluorescence spectroscopy. *Biochem.* **36**: 4535-4541.

Ahmadian MR, Wittinghofer A, Herrmann C. 2002. Fluorescence methods in the study of small GTP-binding proteins. *Methods Mol. Biol*. **189**: 45-63.

Ahmadian MR, Zor T, Vogt D, Kabsch W, Selinger Z, Wittinghofer A, Scheffzek K. 1999. Guanosine triphosphatase stimulation of oncogenic Ras mutants. *Proc. Natl. Acad. Sci.* USA **96**: 7065-7070.

Aoki Y, Niihori T, Narumi Y, Kure S, Matsubara Y. 2008. The RAS/MAPK syndromes: Novel roles of the RAS pathway in human genetic disorders. *Hum. Mutat.* **29**: 992-1006.

Barbacid M. 1990. Ras oncogenes - their role in neoplasia. *Eur. J. Clin. Invest.* **20**: 225-235.

Boriack-Sjodin PA, Margarit SM, Bar-Sagi D, Kuriyan J. 1998. The structural basis of the activation of Ras by Sos. *Nature* **394**: 337-343.

Bos JL. 1989. Ras oncogenes in human cancer: a review. *Cancer Res.* **49**: 4682-4689.

Bos JL, Rehmann H, and Wittinghofer A. 2007. GEFs and GAPs: Critical elements in the control of small G proteins. *Cell* **129,** 865-877.

Brooks BR, Bruccoleri RE, Olafson D, States DJ, Swaminathan S, Karplus M. 1983. Charmm - a program for macromolecular energy, minimization, and dynamics calculations. *J. Comput. Chem.* **4**: 187-217.

Buhrman G, de Serrano V, Mattos C. 2003. Organic solvents order the dynamic switch II in Ras crystals. *Structure* **11**: 747-751.

Buhrman G, Wink G, Mattos C. 2007. Transformation efficiency of RasQ61 mutants linked to structural features of the switch regions in the presence of Raf. *Structure* **15**: 1618-1629.

Bunney TD, Harris R, Gandarillas NL, Josephs MB, Roe SM, Sorli SC, Paterson HF, Rodrigues-Lima F, Esposito D, Ponting CP, Gierschik P, Pearl LH, Driscoll PC, Katan M. 2006. Structural and mechanistic insights into ras association domains of phospholipase C epsilon. *Mol. Cell* **21**: 495-507.

Carta C, Pantaleoni F, Bocchinfuso G, Stella L, Vasta I, Sarkozy A, Digilio C, Palleschi A, Pizzuti A, Grammatico P, Zampino G, Dallapiccola B, Gelb BD, and Tartaglia M. 2006. Germline missense mutations affecting KRAS isoform B are associated with a severe Noonan syndrome phenotype. *Am. J. Hum. Genet.* **79**: 129-135.

Chung HH, Benson DR, and Schultz PG. 1993. Probing the structure and mechanism of Ras protein with an expanded genetic code. *Science* **259**: 806-809.

Cirstea IC, Kutsche K, Dvorsky R, Gremer L, Carta C, Horn D, Roberts AE, Lepri F, Merbitz-Zahradnik T, Konig R, Kratz CP, Pantaleoni F, Dentici ML, Joshi VA, Kucherlapati RS, Mazzanti L, Mundlos S, Patton MA, Silengo MC, Rossi C et al. 2010. A restricted spectrum of NRAS mutations causes Noonan syndrome. *Nat. Genet.* **42**: 27-29.

Denayer E, Parret A, Chmara M, Schubbert S, Vogels A, Devriendt K, Frijns JP, Rybin V, De Ravel TJ, Shannon K, Cools J, Scheffzek K, Legius E. 2008. Mutation analysis in Costello syndrome: Functional and structural characterization of the HRAS p.Lys 117Arg mutation. *Hum. Mutat.* **29**: 232-239.

Der CJ. 1989. The ras family of oncogenes. *Cancer Treat. Res*. **47**: 73-119.

Der CJ, Finkel T, Cooper GM. 1986. Biological and biochemical properties of human rasH genes mutated at codon 61. *Cell* **44**: 167-176.

Eberth A, Dvorsky R, Becker CFW, Beste A, Goody RS, Ahmadian MR. 2005. Monitoring the real-time kinetics of the hydrolysis reaction of guanine nucleotide-binding proteins. *Biol. Chem*. **386**: 1105-1114.

Estep AL, Tidyman WE, Teitell MA, Cotter PD, Rauen KA. 2006. HRAS mutations in Costello syndrome: Detection of constitutional activating mutations in codon 12 and 13 and loss of wild-type allele in malignancy. *Am. J. Med. Genet. A* **140**: 8-16.

Fiegen D, Dvorsky R, Ahmadian MR. 2006. Structural principles of Ras interaction with regulators and effectors. In: Proteins and Cell Regulation, Kluwer Academic Publishers, Dordrecht, The Netherlands (C. J. Der, editor).

Ford B, Skowronek K, Boykevisch S, Bar-Sagi DB, Nassar N. 2005. Structure of the G60A mutant of Ras. *J. Biol. Chem.* **280**: 25697-25705.

Ford B, Hornak V, Kleinman H, Nassar N. 2006. Structure of a transient intermediate for GTP hydrolysis by ras. *Structure* **14**: 427-436.

Franken SM, Scheidig AJ, Krengel U, Rensland H, Lautwein A, Geyer M, Scheffzek K, Goody RS, Kalbitzer HR, Pai EF, et al. 1993. Three-dimensional structures and properties of a transforming and a nontransforming glycine-12 mutant of p21H-ras. *Biochem.* **32**: 8411-8420.

Gasper R, Thomas C, Ahmadian MR, Wittinghofer A. 2008. The role of the conserved switch II glutamate in guanine nucleotide exchange factor-mediated nucleotide exchange of GTP-binding proteins. *J. Mol. Biol.* **379**: 51-63.

Gelb BD, Tartaglia M. 2006. Noonan syndrome and related disorders: dysregulated RAS-mitogen activated protein kinase signal transduction. *Hum. Mol. Genet.* **15**: R220-R226.

Gremer L, De Luca A, Merbitz-Zahradnik T, Dallapiccola B, Morlot S, Tartaglia M, Kutsche K, Ahmadian MR, Rosenberger G. 2010. Duplication of Glu^{37} in the switch I region of HRAS impairs effector/GAP binding and underlies Costello syndrome by promoting

enhanced growth factor-dependent MAPK and AKT activation. *Hum. Mol. Genet.* **19**: 790-802.

Gremer L, Gilsbach B, Ahmadian MR, Wittinghofer A. 2008. Fluoride complexes of oncogenic Ras mutants to study the Ras-RasGAP interaction. *Biol. Chem*. **389**: 1163-1171.

Gripp KW, Lin AE, Stabley DL, Nicholson L, Scott CI, Doyle D, Aoki Y, Matsubara Y, Zackai EH, Lapunzina P, Gonzalez-Meneses A, Holbrook J, Agresta CA, Gonzalez IL, and Sol-Church K. 2006. HRAS mutation analysis in Costello syndrome: Genotype and phenotype correlation. *Am. J. Med. Genet. A* **140**: 1-7.

Guo Z, Ahmadian MR, Goody RS. 2005. Guanine nucleotide exchange factors operate by a simple allosteric competitive mechanism. *Biochem*. **44**: 15423-15429.

Hall BE, Bar-Sagi D, Nassar N. 2002. The structural basis for the transition from Ras-GTP to Ras-GDP. *Proc. Natl. Acad. Sci. USA* **99**: 12138-12142.

Hemsath L, Ahmadian MR. 2005. Fluorescence approaches for monitoring interactions of Rho GTPases with nucleotides, regulators, and effectors. *Methods* **37**: 173-182.

Herbrand U, Ahmadian MR. 2006. p190-RhoGAP as an integral component of the Tiam1/Rac1-induced downregulation of Rho. *Biol. Chem*. **387**: 311-317.

Herrmann C. 2003. Ras-effector interactions: after one decade. *Curr. Opin. Struct. Biol.* **13**: 122-129.

Herrmann C, Martin GA, Wittinghofer A. 1995. Quantitative analysis of the complex between p21ras and the Ras-binding domain of the human Raf-1 protein kinase. *J. Biol. Chem.* **270**: 2901-2905.

Huang L, Hofer F, Martin GS, Kim SH. 1998. Structural basis for the interaction of Ras with RalGDS. *Nat. Struct. Biol.*, **5**: 422-426.

Hwang MCC, Sung YJ, Hwang YW. 1996. The differential effects of the Gly-60 to Ala mutation on the interaction of H-Ras p21 with different downstream targets. *J. Biol. Chem.* **271**: 8196-8202.

Ito Y, Yamasaki K, Iwahara J, Terada T, Kamiya A, Shirouzu M, Muto Y, Kawai G, Yokoyama S, Laue ED, Wälchli M, Shibata T, Nishimura S, Miyazawa T. 1997. Regional polysterism in the GTP-bound form of the human c-Ha-Ras protein. *Biochem.* **36**: 9109-9119.

Karnoub AE, Weinberg RA. 2008. Ras oncogenes: split personalities. *Nat. Rev. Mol. Cell. Biol.* **9**: 517-531.

Kigawa T, Yamaguchi-Nunokawa E, Kodama K, Matsuda T, Yabuki T, Matsuda N, Ishitani R, Nureki O, Yokoyama S. 2002. Selenomethionine incorporation into a protein by cell-free synthesis. *J. Struct. Funct. Genomics* **2**: 29-35

Klink BU, Goody RS, Scheidig AJ. 2006. A newly designed microspectrofluorometer for kinetic studies on protein crystals in combination with x-ray diffraction. *Biophys. J.* **91**: 981-992.

Kranenburg O. 2005. The KRAS oncogene: past, present, and future. *Biochim. Biophys. Acta* **1756**: 81-82.

Kratz CP, Niemeyer CM, Zenker M. 2007. An unexpected new role of mutant Ras: perturbation of human embryonic development. *J. Mol. Med.* **85**: 223-231.

Kraulis PJ, Domaille PJ, Campbell-Burk SL, Van Aken T, Laue ED. 1994. Solution structure and dynamics of ras p21.GDP determined by heteronuclear three- and four-dimensional NMR spectroscopy. Biochem. 33: 3515-3531.

Krengel, U. 1991. Struktur und Guanosintriphosphathydrolysemechanismus des C-terminal verkürzten menschlichen Krebsproteins P21-H-RAS. PhD. thesis, Heidelberg

Krengel U, Schlichting I, Scherer A, Schumann R, Frech M, John J, Kabsch W, Pai EF, Wittinghofer A. 1990. Three-dimensional structures of H-ras p21 mutants: molecular basis for their inability to function as signal switch molecules. *Cell* **62**: 539-548.

Lenzen C, Cool RH, Prinz H, Kuhlmann J, Wittinghofer A. 1998. Kinetic analysis by fluorescence of the interaction between Ras and the catalytic domain of the guanine nucleotide exchange factor Cdc25Mm. *Biochem.* **37**: 7420-7430.

Lo FS, Lin JL, Kuo MT, Chiu PC, Shu SG, Chao MC, Lee YJ, Lin SP. 2009. Noonan syndrome caused by germline KRAS mutation in Taiwan: report of two patients and a review of the literature. *Eur. J. Pediat.* **168**: 919-923.

Malumbres M, Barbacid M. 2003. RAS oncogenes: The first 30 years. *Nat. Rev. Cancer* **3**: 708.

Margarit SM, Sondermann H, Hall BE, Nagar B, Hoelz A, Pirruccello M, Bar-Sagi D, Kuriyan J. 2003. Structural evidence for feedback activation by Ras.GTP of the Ras-specific nucleotide exchange factor SOS. *Cell* **112**: 685-695.

Milburn MV, Tong L, deVos AM, Brunger A, Yamaizumi Z, Nishimura S, Kim SH. 1990. Molecular switch for signal transduction: structural differences between active and inactive forms of protooncogenic ras proteins. *Science* **247**: 939-945.

Nassar N, Horn G, Herrmann C, Scherer A, McCormick F, Wittinghofer A. 1995. The 2.2 A crystal structure of the Ras-binding domain of the serine/threonine kinase c-Raf1 in complex with Rap1A and a GTP analogue. *Nature* **375**: 554-560.

Nava C., Hanna N., Michot C., Pereira S., Pouvreau N., Niihori T., Aoki Y., Matsubara Y., Arveiler B., Lacombe D., Pasmant E., Parfait B., Baumann C., Heron D., Sigaudy S., Toutain A., Rio M., Goldenberg A., Leheup B., Verloes A. et al. 2007. Cardio-facio-cutaneous and Noonan syndromes due to mutations in the RAS/MAPK signalling pathway: genotype-phenotype relationships and overlap with Costello syndrome. *J. Med. Genet.* **44**: 763-771.

Niihori T, Aoki Y, Narumi Y, Neri G, Cave H, Verloes A, Okamoto N, Hennekam RCM, Gillessen-Kaesbach G, Wieczorek D, Kavamura MI, Kurosawa K, Ohashi H, Wilson L, Heron D, Bonneau D, Corona G, Kaname T, Naritomi K, Baumann C et al. 2006. Germline KRAS and BRAF mutations in cardio-facio-cutaneous syndrome. *Nat. Genet.* **38**: 294-296.

Pacold ME, Suire S, Perisic O, Lara-Gonzalez S, Davis CT, Walker EH, Hawkins PT, Stephens L, Eccleston JF, Williams RL. 2000. Crystal structure and functional analysis of Ras binding to its effector phosphoinositide 3-kinase gamma. *Cell* **103**: 931-943.

Pai EF, Krengel U, Petsko GA, Goody RS, Kabsch W, Wittinghofer A. 1990. Refined crystal structure of the triphosphate conformation of H-ras p21 at 1.35 A resolution: implications for the mechanism of GTP hydrolysis. *EMBO J.* **9**: 2351-2359.

Pechlivanis M, Ringel R, Popkirova B, Kuhlmann J. 2007. Prenylation of Ras facilitates hSOS1-promoted nucleotide exchange, upon Ras binding to the regulatory site. *Biochem*. **46**: 5341-5348.

Quilliam LA, Zhong S, Rabun KM, Carpenter JW, South TL, Der CJ, Campbellburk S. 1995. Biological and structural characterization of a Ras transforming mutation at the phenylalanine-156 residue, which is conserved in all members of the Ras superfamily. *Proc. Natl. Acad. Sci.* USA. **92**: 1272-1276.

Quinlan MP, Settleman J. 2009. Isoform-specific ras functions in development and cancer. *Future Oncol.* **5**: 105-116.

Reinstein J, Schlichting I, Frech M, Goody RS, Wittinghofer A. 1991. p21 with a phenylalanine 28-leucine mutation reacts normally with the GTPase activating protein GAP but nevertheless has transforming properties. *J. Biol. Chem.* **266**: 17700-17706.

Scheffzek K, Ahmadian MR. 2005. GTPase activating proteins: structural and functional insights 18 years after discovery. *Cell. Mol. Life Sci.* **62**: 3014-3038.

Scheffzek K, Grünewald P, Wohlgemuth S, Kabsch W, Tu H, Wigler M, Wittinghofer A, Herrmann C. 2001. The Ras-Byr2RBD complex: structural basis for Ras effector recognition in yeast. *Structure* **9**: 1043-1050.

Scheffzek K, Ahmadian MR, Kabsch W, Wiesmuller L, Lautwein A, Schmitz F, Wittinghofer A. 1997. The Ras-RasGAP complex: Structural basis for GTPase activation and its loss in oncogenic Ras mutants. *Science* **277**: 333-338.

Scheffzek K, Grunewald P, Wohlgemuth S, Kabsch W, Tu H, Wigler M, Wittinghofer A, Herrmann C. 2001. The Ras-Byr2RBD complex: structural basis for Ras effector recognition in yeast. *Structure* **9,** 1043-1050.

Scheidig AJ, Burmester C, Goody RS. 1999 The pre-hydrolysis state of p21(ras) in complex with GTP: new insights into the role of water molecules in the GTP hydrolysis reaction of ras-like proteins. *Structure* **7**: 1311-1324.

Scheidig AJ, Franken SM, Corrie JE, Reid GP, Wittinghofer A, Pai EF, Goody RS. 1995. X-ray crystal structure analysis of the catalytic domain of the oncogene product p21H-ras complexed with caged GTP and mant dGppNHp. *J. Mol. Biol.* **253**: 132-150.

Scheidig AJ, Sanchez-Llorente A, Lautwein A, Pai EF, Corrie JE, Reid GP, Wittinghofer A, Goody RS. 1994. Crystallographic studies on p21(H-ras) using the synchrotron Laue method: improvement of crystal quality and monitoring of the GTPase reaction at different time points. *Acta Crystallogr. D* **50**: 512-520.

Schubbert S, Shannon K, Bollag G. 2007a. Hyperactive Ras in developmental disorders and cancer. *Nat. Rev. Cancer* **7**: 563.

Schubbert S, Bollag G, Lyubynska N, Nguyen H, Kratz CP, Zenker M, Niemeyer CM, Molven A, Shannon K. 2007b. Biochemical and functional characterization of germ line KRAS mutations. *Mol. Cell. Biol*. **27**: 7765-7770.

Schubbert S, Zenker M, Rowe SL, Boll S, Klein C, Bollag G, van der Burgt I, Musante L, Kalscheuer V, Wehner LE, Nguyen H, West B, Zhang KYJ., Sistermans E, Rauch A, Niemeyer CM, Shannon K, Kratz CP. 2006. Germline KRAS mutations cause Noonan syndrome. *Nat. Genet.* **38**: 331-336.

Schweins T, Scheffzek K, Assheuer R, Wittinghofer A. 1997. The role of the metal ion in the p21ras catalysed GTP-hydrolysis: Mn^{2+} versus Mg^{2+}. *J. Mol. Biol.* **266**:847-856.

Seeburg PH, Colby WW, Capon DJ, Goeddel DV, Levinson AD. 1984. Biological properties of human c-Ha-ras1 genes mutated at codon 12. *Nature* **312**: 71-75.

Sol-Church K, Stabley DL, Nicholson L, Gonzalez IL, Gripp KW. 2006. Paternal bias in parental origin of HRAS mutations in Costello syndrome. *Hum. Mutat.* **27**: 736-741.

Sondermann H, Soisson SM, Boykevisch S, Yang SS, Bar-Sagi D, Kuriyan J. 2004. Structural analysis of autoinhibition in the Ras activator Son of sevenless. *Cell* **19**: 393-405.

Sprang SR. 1997. G protein mechanisms: insights from structural analysis. A*nnu. Rev. Biochem.* **66**: 639-678.

Spoerner M, Herrmann C, Vetter IR, Kalbitzer HR, Wittinghofer A. 2001. Dynamic properties of the Ras switch I region and its importance for binding to effectors. *Proc. Natl. Acad. Sci. USA* **98**: 4944-4949.

Stieglitz B, Bee C, Schwarz D, Yildiz O, Moshnikova A, Khokhlatchev A, Herrmann C. 2008. Novel type of Ras effector interaction established between tumour suppressor NORE1A and Ras switch II. *EMBO J.* **27**: 1995-2005.

Stone JC, Colleton M, Bottorff D. 1993. Effector domain mutations dissociate p21(Ras) effector function and GTPase-activating protein-interaction. *Mol. Cell. Biol.* **13**: 7311-7320.

Sung YJ, Hwang MCC, Hwang YW. 1996. The dominant negative effects of H-Ras harboring a Gly to Ala mutation at position 60. *J. Biol. Chem.* **271**: 30537-30543.

Tanaka T, Williams RL, Rabbitts TH. 2007. Tumour prevention by a single antibody domain targeting the interaction of signal transduction proteins with RAS. *EMBO J.* **26**: 3250-3259.

Tidyman WE, Rauen KA. 2009. The RASopathies: developmental syndromes of Ras/MAPK pathway dysregulation. *Curr. Opin. Genet. Devel.* **19**: 230-236.

Tong LA, de Vos AM, Milburn MV, Kim SH. 1991. Crystal structures at 2.2 A resolution of the catalytic domains of normal ras protein and an oncogenic mutant complexed with GDP. *J. Mol. Biol.* **217**: 503-516.

Tsukuda K, Tanino M, Soga H, Shimizu N, Shimizu K. 2000. A novel activating mutation of the K-ras gene in human primary colon adenocarcinoma. *Biochem. Biophys. Res. Commun.* **278**: 653-658.

Tucker J, Sczakiel G, Feuerstein J, John J, Goody RS, Wittinghofer A. 1986. Expression of p21 proteins in Escherichia coli and stereochemistry of the nucleotide-binding site *EMBO J*. **5**: 1351-1358.

Vetter IR, Linnemann T, Wohlgemuth S, Geyer M, Kalbitzer HR, Herrmann C, Wittinghofer A. 1999. Structural and biochemical analysis of Ras-effector signaling via RalGDS. *FEBS Lett.* **45**: 175-180.

Vetter IR, Wittinghofer A. 2001. Signal transduction - The guanine nucleotide-binding switch in three dimensions. *Science* **294**: 1299-1304.

Xu JA, Baase WA, Baldwin E, Matthews BW. 1998. The response of T4 lysozyme to large-to-small substitutions within the core and its relation to the hydrophobic effect. *Protein Sci.* **7**: 158-177.

Zenker M, Lehmann K, Schulz AL, Barth H, Hansmann D, Koenig R, Korinthenberg R, Kreiss-Nachtsheim M, Meinecke P, Morlot S, Mundlos S, Quante AS, Raskin S, Schnabel D, Wehner LE, Kratz CP, Horn D, Kutsche K. 2007. Expansion of the genotypic and phenotypic spectrum in patients with KRAS germline mutations. *J. Med. Genet.* **44**: 131-135.

Figure Legends

Figure 1 Relative positions of amino acids in KRAS altered in patients with NS, CFCS, and CS. A. Secondary structure elements and conserved motifs of RAS. The α-helices and β-strands are illustrated as cylinders and arrows, respectively. The G-domain of RAS also consists of five conserved motifs (G1-G5; gray boxes) that are responsible for specific and tight nucleotide binding and hydrolysis. Bold lines indicate the position of specific RAS signatures including the hypervariable region (HVR), which is polybasic in KRAS 4B. Amino acids investigated in this study are indicated by arrows. The isoprenylation site of the protein is at the cysteine of the C-terminal CaaX motif. B, C. Solvent accessible surfaces of H-RAS molecules are shown in the inactive GDP-bound state (B) and the active GTP-bound state (C). For clarity, structures are illustrated in three different views. Therefore, central panels are rotated 90° around the vertical axes to the right (left panel) and to the left (right panel). Amino acids altered in patients with NS, CFCS, or CS are color-coded. Dashed arrows depict critical residues buried within the hydrophobic core of the protein.

Figure 2 Cellular levels of the active, GTP-bound forms of germline KRAS mutants. Pull down experiments of GTP-bound KRAS proteins (RAS_{GTP}) were performed in COS-7 cells transiently expressing either $KRAS^{wt}$ or germline KRAS mutants in the presence (A) and in the absence of serum (B). Irrespective of culture conditions almost all KRAS mutants showed an increased GTP-bound level. Purified RAS-GAP, which was added to the cleared cell lysates proved the GAP sensitivity of the mutants (B, lower panel). GAP resistant mutants, RAS^{P34L}, RAS^{P34R} and RAS^{G60R}, resided in the active state comparable to oncogenic RAS^{G12V}. Total amounts of recombinant RAS are shown for equal expression and loading. Anti-RAS antibodies used in these experiments were anti-RAS (RAS10 clone, Upstate-Millipore™, mutants G60R, D153V, F156L) and anti-RAS (BD Transduction Laboratories™,

wt and all other mutants), since some mutations modified the RAS epitope recognized by the respective antibodies. Additional information is given in Supp. Fig. S2.

Figure 3 Modified nucleotide exchange properties of the RAS mutants. Intrinsic (A, B) and GEF-catalysed (C, D) mantGDP dissociation from the RAS proteins (0.2 µM) in the presence of 40 µM GDP (A) or of 40 µM GDP and 2 µM CDC25 (C). On the panels A and C the respective time-dependent reactions of RAS^{wt} and a representative RAS mutant (Q22E) are shown. On the panels B and D the observed rate constant of all RAS proteins are illustrated. RAS^{wt}, RAS^{G12V} and RAS^{F28L} were included as controls. The insets (in A and C) show the complete time course of the mantGDP dissociation from RAS^{wt}. Standard errors of five to seven independent measurements are shown.

Figure 4 GAP insensitivity of the RAS mutants. (A, B) Intrinsic γ^{32}P-GTP hydrolysis reaction rates were measured for individual RAS proteins (1µM). (C, D) GAP-stimulated GTPase reaction of the RAS proteins (0.2 µM) was measured in the presence of 2 µM NF1-333. On the panels A and C the respective time-dependent reactions of RAS^{wt} and a representative RAS mutant (G60R in A, Q22E in C) are shown. RAS^{wt}, RAS^{G12V} and RAS^{F28L} were included as controls. The inset in panel C shows the complete and more detailed time course of GAP activity on RAS^{wt}. Standard errors of five to seven independent measurements are shown.

Figure 5 Increased downstream signaling activity of the germline RAS mutants under serum-free conditions. KRAS mutants, transiently transfected in COS-7 cells were analyzed for the phosphorylation level of MEK (pMEK1/2), ERK (pERK1/2) and AKT (pAKT) under serum-free culture conditions. The amounts of total RAS, MEK, ERK and AKT in the cleared

cell lysates as well as RAS^{wt}, RAS^{G12V} and RAS^{F28L} were included as controls. Results of experiments in the presence of serum are shown in Supp. Fig. S4.

Figure 6 Significant loss of RAF1 binding affinity for RAS mutants. Binding of RAF1-RBD (increasing concentrations as indicated) to mantGppNHp-bound RAS (0.2 µM) was measured using fluorescence polarization. On the panel A, the respective concentration-dependent measurements of RAS^{wt} and a representative RAS mutant (G60R) are shown. On panel B, the dissociation constants (K_d) of all RAS proteins are illustrated. RAS^{wt}, RAS^{G12V} and RAS^{F28L} were included as controls. Data obtained with another RAS effector, RALGDS are shown in Supp. Fig. S5.

Electronic Supporting Information

Germline *KRAS* mutations cause aberrant biochemical and physical properties leading to developmental disorders

Lothar Gremer[1#], Torsten Merbitz-Zahradnik[1#], Radovan Dvorsky[1#], Ion C. Cirstea[1#], Christian Peter Kratz[2], Martin Zenker[3], Alfred Wittinghofer[4] and Mohammad Reza Ahmadian[1*]

[1] Institute of Biochemistry & Molecular Biology II, Medical Faculty, Heinrich-Heine University, Universitaetsstr. 1, 40225 Düsseldorf, Germany; [2] Clinical Genetics Branch, DCEG, NCI, 6120 Executive Boulevard, Room EPS 7030, Rockville, MD 20852; [3] Institute of Human Genetics, University Hospital Magdeburg, Leipziger Str. 44, 39120 Magdeburg, Germany; [4] Max-Planck Institute of Molecular Physiology, Department of Structural Biology, Otto-Hahn-Strasse 11, 44227 Dortmund, Germany;

[#] These authors contributed equally to this work.

Running head: Functional impact of *KRAS* germline mutations

[*] Corresponding author: Institute of Biochemistry & Molecular Biology II
Heinrich Heine University Medical Center
Universitätsstr. 1
40225 Düsseldorf
Germany
Phone: #49 211 811 2384
Fax: #49 211 811 2726
E-mail: Reza.Ahmadian@uni-duesseldorf.de

Table S1 *Overview of RAS structures*

GTPase	Nucleotide[a]	Resolution (Å)	PDB code	References
$HRAS^{wt}$	Gpp(NH)p	1,35	5p21	Pai et al. 1990
$HRAS^{wt}$	$Gpp(CH_2)p$	1.54	121p	Krengel, 1991
$HRAS^{wt}$	$Gpp(CH_2)p$	1.95	6q21	Milburn et al. 1990
$HRAS^{wt}$	Gpp(NH)p, GTP	1.35, 1.60	1ctq, 1qra	Scheidig et al. 1999
$HRAS^{wt}$	caged-GTP	1.85, 2.50	1gnr, 1gnq	Scheidig et al. 1995
$HRAS^{wt}$	mantGpp(NH)p	2.70	1gnp	Scheidig et al. 1995
$HRAS^{wt}$	Gpp(NH)p	2.0, 2.0, 2.30, 2.45	1p2t, 1p2u, 1p2v, 1p2s	Buhrman et al. 2003
$HRAS^{wt}$	Gpp(NH)p	1.40	2rge	Buhrman et al. 2007
$HRAS^{G12D}$	Gpp(NH)p	2.30	1agp	Franken et al. 1993
$HRAS^{G12P}$	Gpp(NH)p	1.50	821p	Franken et al. 1993
$HRAS^{G12P}$	$Gpp(CH_2)p$	1.80	1jai	Schweins et al. 1997
$HRAS^{G12P}$	GTP	2.80	1plk	Scheidig et al. 1994
$HRAS^{G12R}$	Gpp(NH)p	2.20	421p	Krengel et al. 1990
$HRAS^{G12P}$	caged-GTP	2.80	1plj	Scheidig et al. 1994
$HRAS^{G12V}$	GTP	2.60	521p	Krengel et al. 1990
$HRAS^{G12V}$	DABP-Gpp(NH)p	1.90; 1.70	1rvd; 1clu	Ahmadian et al. 1999
$HRAS^{G12V,A122G}$	$Gpp(CH_2)p$	1.80	1jah	Schweins et al. 1997
$HRAS^{Y32C,C118S}$	caged-GTP	1.05, 1.24	2evw, 2cl6	Klink et al. 2006
$HRAS^{Y32C,C118S}$	GTP	1.25, 1.30	2cl7, 2clc	Klink et al. 2006
$HRAS^{Y32C,C118S}$	Gpp(NH)p	1.80	2cl0	Klink et al. 2006
$HRAS^{T35S}$	Gpp(NH)p	2.90	1iaq	Spoerner et al. 2001
$HRAS^{D38E}$	Gpp(NH)p	2.30	221p	Krengel et al. 1990
$HRAS^{T50I}$	Gpp(NH)p	1.36	3i3s	Cirstea et al.2010
$HRAS^{A59G}$	GTP	1.70	1lf0	Hall et al. 2002
$HRAS^{G60A}$	Gpp(NH)p	1.84	1xcm	Ford et al. 2005
$HRAS^{Q61G}$	GTP	1.50	1zw6	Ford et al. 2006
$HRAS^{Q61H}$	Gpp(NH)p	2.40	621p	Krengel et al. 1990
$HRAS^{Q61I}$	Gpp(NH)p	1.90, 1.45	2rga, 2rgg	Buhrman et al. 2007
$HRAS^{Q61K}$	Gpp(NH)p	1.35	2rgb	Buhrman et al. 2007
$HRAS^{Q61L}$	Gpp(NH)p	2.00	721p	Krengel et al. 1990
$HRAS^{Q61L}$	Gpp(NH)p	2.00	2rgd	Buhrman et al. 2007
$HRAS^{Q61V}$	Gpp(NH)p	1.60	2rgc	Buhrman et al. 2007
$HRAS^{wt}$	GDP	2.00	4q21	Milburn et al. 1990
$HRAS^{wt}$	GDP	2.00	1ioz	Kigawa et al. 2001
$HRAS^{wt}$	GDP	2.20	1q21	Tong et al. 1991
$HRAS^{wt}$	GDP	NMR	1crp, 1crq, 1crr	Kraulis et al. 1994
$HRAS^{wt}$	GDP	NMR	1aa9	Ito et al. 1997
$HRAS^{G12V}$	GDP	2.20	2q21	Tong et al. 1991
$HRAS^{G12P}$	GDP	2.80	1pll	Scheidig et al. 1994
$HRAS^{Y32C,C118S}$	GDP	1.00	2ce2	Klink et al. 2006
$HRAS^{A59G}$	GDP	1.70	1lf5	Hall et al. 2002
$HRAS^{G60A}$	GDP	1.70	1xj0	Ford et al. 2005
$HRAS^{Q61G}$	GDP	2.00	1zvq	Ford et al. 2006
$HRAS^{K117R}$	GDP	1.49	2quz	Denayer et al. 2008
$HRAS^{C118S}$	GDP	1.22	2cld	Klink et al. 2006
$HRAS^{I163F}$	GDP	1.70	2x1v	Anand et al. 2010 [b]
$KRAS^{Q61H,\ R151G}$	Gpp(NH)p	2.27	3gft	Tong et al. 2009 [b]
$NRAS^{wt}$	GDP	1.65	3con	Nedyalkova et al. 2008 [b]

[a] Non-hydrolysable GTP analogs: caged-GTP, P3-1-(2-nitro) phenylethyl guanosine 5′-O-triphosphate; $Gpp(CH_2)p$, guanosine 5´-β,γ-methylene-diphosphonate; Gpp(NH)p, guanosine imidotriphosphate; DAPB-Gpp(NH)p, diaminobenzophenone-Gpp(NH)p; mantGpp(NH)p, fluorescent N-methylanthraniloyl-Gpp(NH)p. [b] unpublished data

Table S2 *Overview of RAS structures in the complex with regulators and effectors*

GTPase	Nucleotide[a]	Resolution (Å)	PDB code	partner	References
RAP^{wt}	Gpp(NH)p	1,90	1C1Y	RAF1	Nassar et al. 1995
$HRAS^{wt}$	Gpp(NH)p	3.00	1k8r	BYR2	Scheffzek et al. 2001
$HRAS^{G12V}$	Gpp(NH)p	3.00	1he8	PI3Kγ	Pacold et al. 2000
$HRAS^{G12V}$	GTP	1.90	2c5l	PLCε	Bunney et al. 2006
$HRAS^{E31K}$	Gpp(NH)p	2.10	1lfd	RALGDS	Huang et al. 1998
$HRAS^{D30E, E31K}$	Gpp(NH)p	1.80	3ddc	NORE1A	Stieglitz et al. 2008
$HRAS^{wt}$	GDP·AlF_3	2.50	1wq1	$p120^{RASGAP}$	Scheffzek et al. 1997
$HRAS^{wt}$	no	2.80	1bkd	SOS1	Boriack-Sjodin et al. 1998
$HRAS^{A59G}$	GTP	3.20	1nvx	SOS1	Margarit et al. 2003
$HRAS^{wt}$	Gpp(NH)p	2.70	1nvw	SOS1	Margarit et al. 2003
$HRAS^{A59G}$	Gpp(NH)p	2.20	1nvu	SOS1	Margarit et al. 2003
$HRAS^{Y64A}$	Gpp(NH)p	2.18	1nvv	SOS1	Margarit et al. 2003
$HRAS^{Y64A}$	GDP	2.70	1xd2	SOS1	Sondermann et al. 2004
$HRAS^{G12V}$	GTP	2.00	2uzi	Anti-Ras FV	Tanaka et al. 2007
$HRAS^{G12V}$	GTP	2.70	2vh5	Anti-Ras FV	Tanaka et al. 2007

[a] Gpp(NH)p (non-hydrolysable GTP analogs), guanosine imidotriphosphate; GDP·AlF3, guanosine diphosphate-aluminium fluoride mimics the transition state of the GTP hydrolysis reaction; "no" stands for nucleotide-free.

Table S3 *Calculated structural parameters of amino acid residues altered in NS, CFC and CS patients*

	Solvent accessible surface[a] (Å^2)			Nucleotide vicinity[b] (Å)	Protein partner contact[c] (Å)						
Residue	GDP	GTP	DEV	AVR	GAP	SOS_1	SOS_2	PI3Kγ	BYR2	RalGDS	PCLε
K5	58.2	64.3	6.2	17.02	8.09	6.81	8.05	8.20	4.79	10.43	8.03
V14	**0.0**	**5.5**	5.5	**3.36**	6.26	7.12	11.52	13.78	14.55	13.60	13.84
Q22	11.9	17.5	5.6	7.99	8.96	5.44	4.28	7.69	10.55	9.55	9.04
P34	82.1	78.3	3.8	3.83	**3.42**	**3.22**	**2.69**	6.00	6.04	**3.44**	4.85
T58	25.0	**4.5**	20.5	4.25	7.86	**3.92**	8.27	8.85	9.37	8.70	8.79
G60	52.8	25.6	27.3	**3.34**	4.76	**2.88**	6.56	11.45	11.37	10.41	10.69
E153	56.7	59.8	3.1	11.22	16.98	14.67	**2.59**	15.77	15.91	14.78	14.38
F156	**0.0**	**0.0**	0.0	10.80	12.94	9.43	9.46	12.00	11.76	11.31	11.69

[a] Solvent accessible surface area was calculated using the structures of the inactive, GDP-bound (PDB code 4Q21) and the active, GTP-bound (1CTQ) forms of HRAS. Boldface indicates residues with lowest accessible surface area.
[b] Nucleotide vicinity highlights the minimal distance of amino acid side chain to the nucleotide (GDP or GTP). Boldface indicates residues that are in direct contact with the nucleotide.
[c] Protein partner contact highlights the minimal distance of amino acid side chain to the interacting partners (GAP, GEF, Effector). Boldface indicates residues that are in direct contact with the interacting partners. Following structures were analyzed: GAP (1WQ1), SOS (1NVV), PI3K (1HE8), BYR2 (1K8R), RalGDS (1LFD) and Phospholipase C epsilon (2C5L). Two RAS molecules from the structure of RAS-SOS1 complex were considered: SOS_1 is nucleotide-free RAS in the complex with the CDC25 domain and SOS_2 is RAS·GTP in complex with the REM domain.
DEV (deviation) describes differences between the two states. Average (AVR) values are calculated from nine nucleotide-bound HRAS structures.

Table S4 *Summary of biochemical properties of the RAS proteins*

Groups	RAS mutant	mant-GppNHP association	Intrinsic mantGDP dissociation	GEF-catalyzed mantGDP dissociation	Intrinsic GTPase	GAP-stimulated GTPase	RAF-RBD binding
controls	wt	1	1	1	1	1	1
	G12V	**7.89**	0.67	0.56	**0.16**	**0.00**	**0.190**
	F28L	**19.21**	5.00	**9.78**	0.57	**0.10**	**0.030**
A	K5N	0.2	1.33	1.22	1.01	1.11	1.375
	T58I	3.68	4.33	1.67	0.58	0.88	0.158
	E153V	0.34	1.67	2.22	0.47	0.87	0.373
B	V14I	0.74	**29.67**	**19.67**	1.08	1.16	0.162
C	Q22R	0.55	1.33	2.22	0.69	**0.04**	0.431
D	Q22E	0.37	**26.00**	**23.33**	1.11	**0.03**	0.156
	F156L	0.66	**63.33**	**33.11**	0.85	**0.03**	**0.044**
E	P34L	1.84	2.67	1.56	0.99	**0.00**	**0.008**
	P34R	2.37	2.00	0.67	0.96	**0.00**	**0.009**
	G60R	0.63	1.33	**0.00**	**0.08**	**0.00**	**0.019**

Biochemical data of the RAS mutants are calculated in relation to RAS^{wt}. All relative rates are given in k_{obs} (mut) devided by k_{obs} (wt), which corresponds to a reversed binding affinity of RAF-RBD. Green color outlines effects that favor increased signaling, red those impaired signaling, such as lower affinity of effectors. Based on our biochemical data, RAS mutants are grouped into different functional classes: (A) no major changes; (B) increase in intrinsic and catalyzed nucleotide exchange; (C) decrease in GAP-stimulated GTPase; (D) increase in intrinsic and catalyzed nucleotide exchange and decreased in GAP-stimulated GTPase; (E) defective interaction with GAPs and effectors and also with GEFs in the case of RAS^{G60R}.

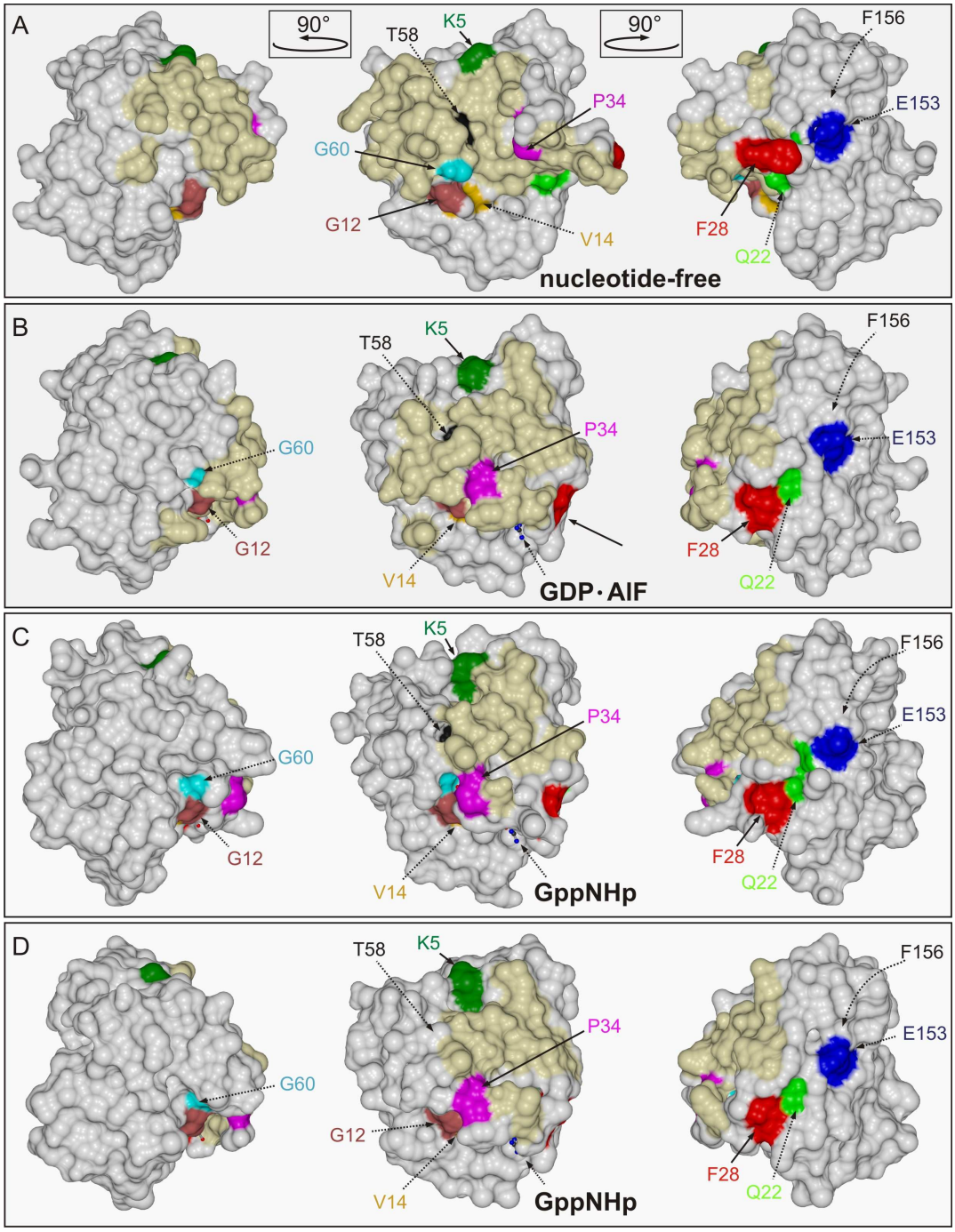

Figure S1 Almost all mutational sites are located outside the interacting interface. Relative positions of amino acids in KRAS altered in patients with NS, CFCS, and CS are highlighted with respect to its interaction with CDC25 (A), GAP-334 (B), RAF-RBD (C) and RALGDS-RBD (D). For clarity, structures are illustrated in three different views. Therefore, central panels are rotated 90° around the vertical axes to the right (left panel) and to the left (right panel). The contact region of the binding partners of RAS (GEFs, GAPs and effectors) are highlighted in pale yellow. Amino acids altered in patients with NS, CFCS, or CS are color-coded. Dashed arrows depict critical residues buried within the hydrophobic core of the protein.

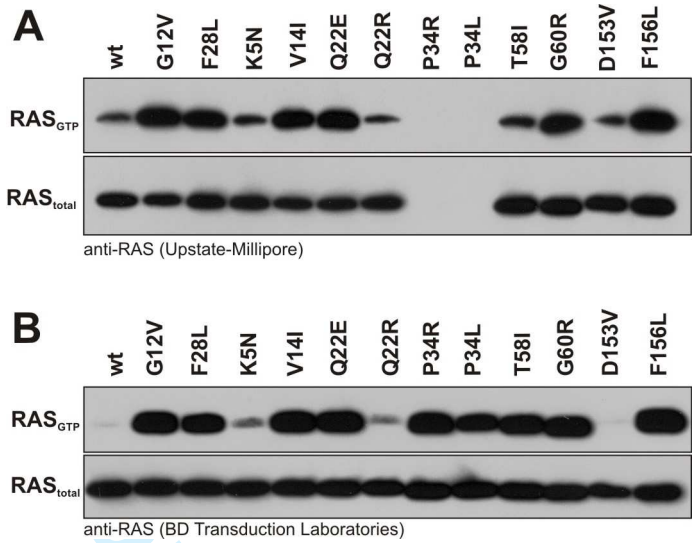

Figure S2 Germline RAS mutants mostly reside in the GTP-bound state. These experiments have been performed under the same conditions as in Figure 2 except for the anti-RAS antibodies. Two different antibodies were employed in order to investigate the impact of the RAS point mutation on antibody recognition since mutated residues can potentially alter epitopes. In (A) anti-RAS from Upstate-Millipore™ (clone RAS10) was applied, in panel B anti-RAS from BD Transduction Laboratories™ (No. 61002) was used. The detection of KRAS^{P34L} and KRAS^{P34R} by the Upstate-Millipore™ antibody (A) was impaired, whereas the detection of the KRAS^{D153V}, but only in the active GTP state (B) was impaired by the BD Transduction Laboratories™ antibody, which is most likely due to epitope changes derived by the respective mutations. Total amounts of recombinant RAS are applied for equal expression and loading.

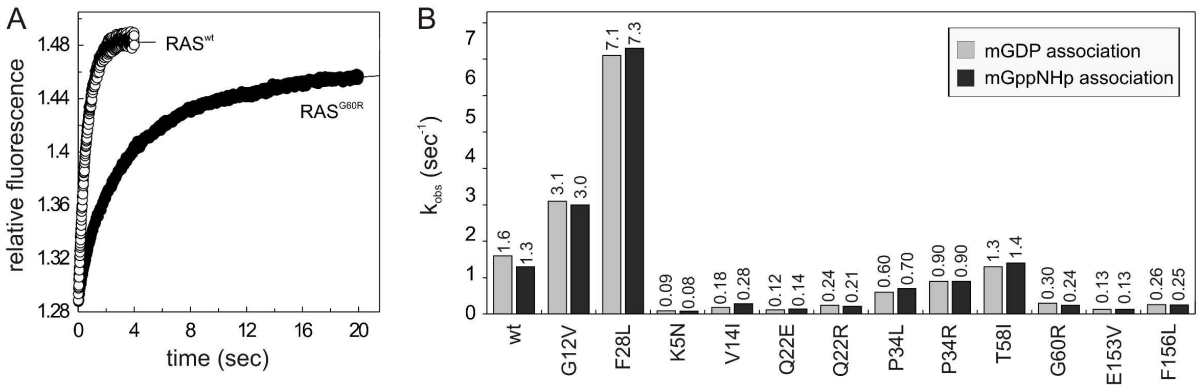

Figure S3 Reduced nucleotide association by germline RAS mutants. (A) time-dependent association reactions of fluorescent nucleotide (0.2 µM) with nucleotide-free RAS proteins (0.3 µM; RAS^{wt} and a representative RAS mutant, G60R) are shown. (B) Observed rate constants (k_{obs}) of all RAS mutants, as measured in (A) are illustrated. RAS^{wt}, RAS^{G12V} and RAS^{F28L} were included as controls. All data shown are an average of five to seven different experiments. Interestingly and in contrast to oncogenic mutation G12V, the association rates of fluorescently labeled GDP (mantGDP) or a non-hydrolyzable fluorescently labeled GTP analog (mantGppNHp) with all other RAS mutants are comparable or slower then that of wild type reaching a maximum 20-fold difference in the case of K5N. All mutants show, as RAS^{wt}, no preference for a particular nucleotide. However, the difference in association kinetics of the RAS mutants would not lead to functional consequences due to the high affinity of guanine nucleotides towards RAS and their high concentration in the cell. All data are averages of five to seven independent measurements with a standard deviation of less than 5 %.

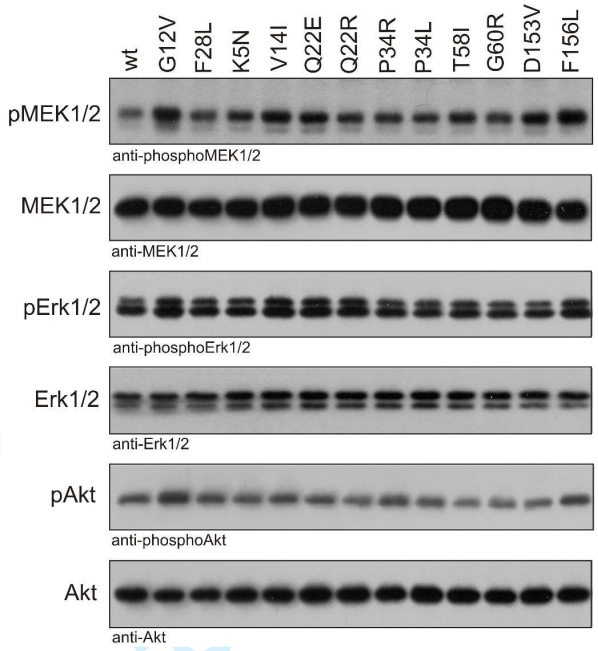

Figure S4 Serum-dependent downstream signaling activity of the germline RAS mutants. MEK, ERK and AKT phosphorylation levels (pMEK1/2, pERK1/2 and pAKT) were determined in transiently transfected COS-7 cells under the same condition as in Figure 5 but cultured in the presence of serum. Total amounts of MEK, ERK and AKT in cell lysates are shown for equal protein expression and loading.

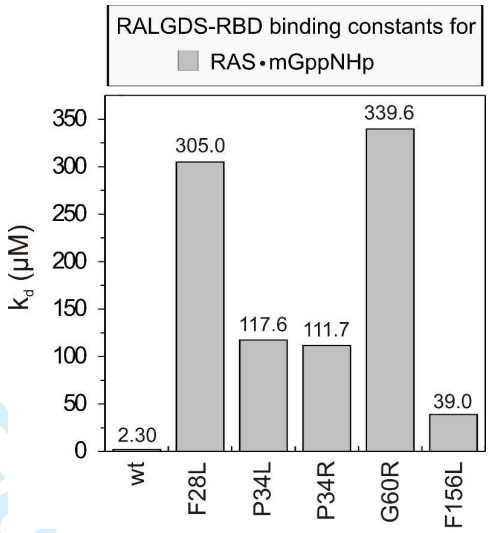

Figure S5 Reduced binding affinity for the RALGDS-RBD interaction with the mantGppNHp-bound RAS mutants. These experiments were performed under the same conditions as for the RAF-RBD (Fig. 6). Only mutants are shown, which revealed significant difference in the RAF-RBD interaction assay (shown in Fig. 6) compared to RAS^{wt}.

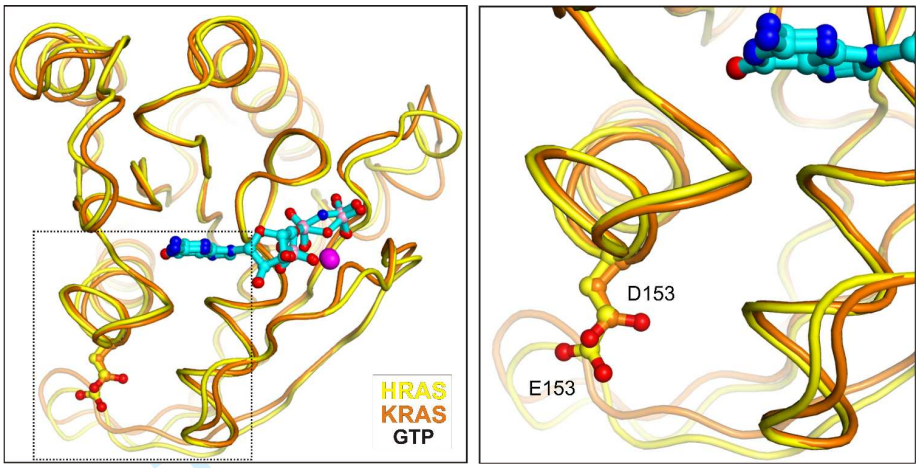

Figure S6 Structural identity of KRAS and HRAS. Left panel, showing superimposed structures of GppNHp-bound HRAS^{wt} (yellow) (Pai et al., 1990) and KRAS$^{Q61H,\ R151G}$ (orange) (Tong et al., 2009; Table S1), demonstrates that both structures are very similar with average RMS deviations between Cα atoms being 0.68 Å. Right panel highlights location of D153 in KRAS, which corresponds to a glutamate in HRAS (see also the box at the left panel). All other KRAS residues that are mutated in patients with NS and related diseases show a similar orientation and conformation. This legitimates our *in vitro* data of *KRAS* mutations using HRAS proteins and their discussion using HRAS structures.

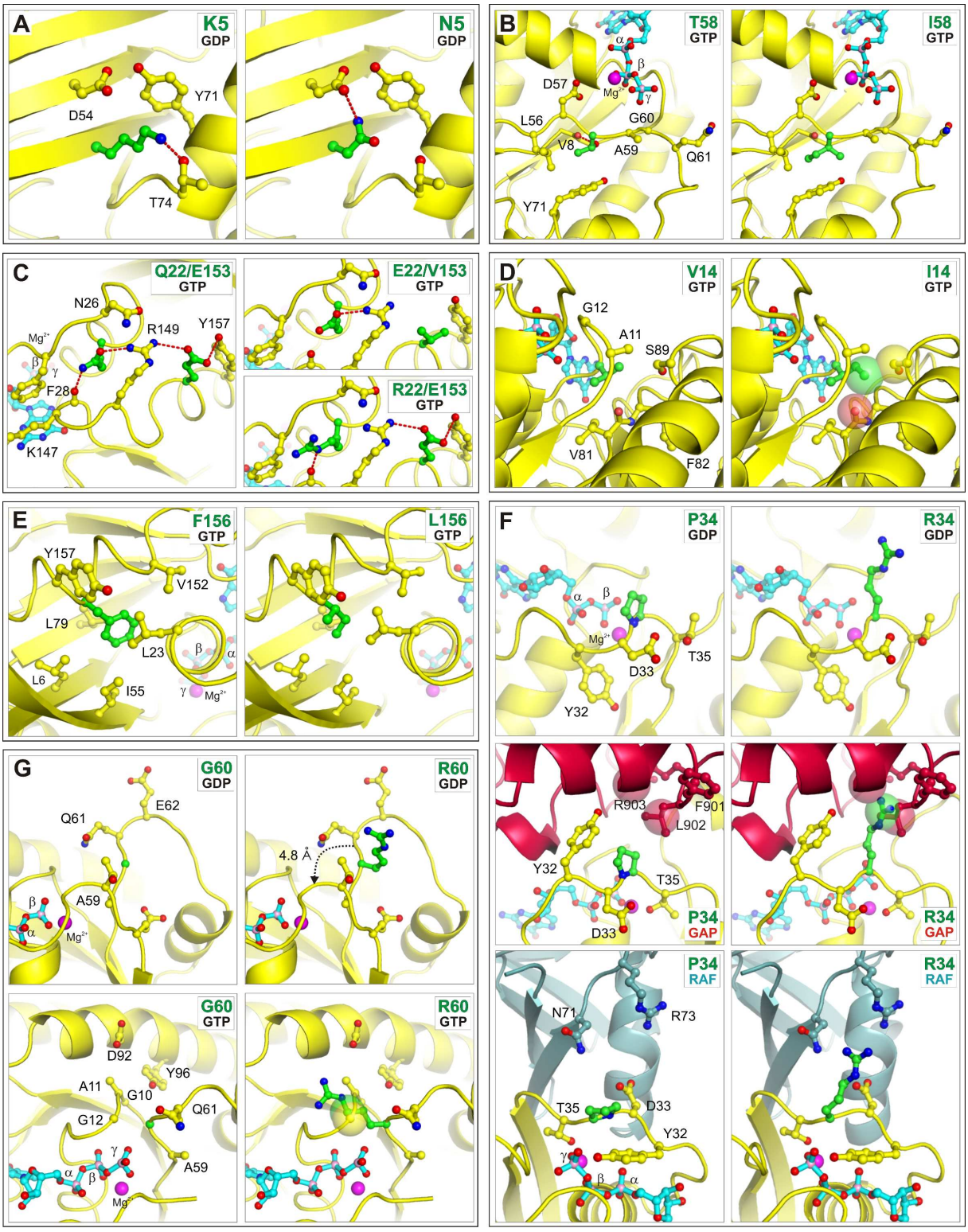

Figure S7 Schematic representation of the structural environment of amino acids altered in patients with NS, CFCS, and CS. Wild-type (left panels) and altered (right panels) residues (in green) are shown on the basis of HRAS structures (Pai et al., 1990; Milburn et al., 1990). Mutant structures were modelled using the CHARMM program (Brooks et al., 1983). (A) K5 is an integral part of a network in GDP- but not in GTP-bound state. Its substitution by an asparagine may indirectly affect nucleotide binding. (B) T58 is surrounded by several critical residues of the switch II. An isoleucine instead of T58 may result in an

increase of flexibility of the switch regions and thus may explain a decrease in nucleotide dissociation. (C) Q22 and E153 (D153 in KRAS4B), located at the edge of the interacting interface of RAS, are involved in a network of intramolecular interactions. Changes at these positions destabilize F28, K147, and R149 and may contribute to faster nucleotide dissociation. In contrast to glutamate at position Q22, which makes new interactions and induces local structural changes, the guanidinium group of an arginine is completely solvent exposed that may counteract GAP binding. (D) V14 substitution by isoleucine generates a steric clash (highlighted as van der Waals spheres), which may change the proper position of the critical G12 residue in the P-loop and consequently, the reaction of GTP hydrolysis. (E) F156 is located in a hydrophobic pocket of RAS formed by surrounding residues. Its substitution by leucine may generate a cavity within the hydrophobic core of the protein leading to conformational changes that may result in overall changes of the intrinsic functions of RAS. (F) P34 does not change its solvent exposed area upon nucleotide exchange and occupies a central position at the contacting surface of the GTP-bound state of RAS. Its substitution to leucine or arginine may result in a direct clash with RAS binding to GAP (red) and effector (light blue). (G) G60 is exposed at the surface in the inactive, GDP-bound state (see arginine at this position). Upon GDP/GTP exchange it turns and shifts by 4.8 Å (see arrow) and is completely buried in the GTP-bound state as illustrated. Substitution of G60 to arginine leads very likely to the collision with catalytical G12 in the GTP-bound (highlighted as van der Waals spheres of G12 and R60 side chain) disturbing the functionality of KRAS.

Assessment of possible structural consequences of RAS mutants

Class A mutants ($KRAS^{K5N}$, $KRAS^{T58I}$, $KRAS^{D153V}$): These mutants exhibit only minor alterations in their *in vitro* biochemical behaviour compared to $KRAS^{wt}$.

K5 is located at the very N-terminus of RAS and creates a hydrophobic contact with Y71 and an ionic contact with N74 in the GDP-bound state (Supp. Fig. S7A). Thus, its substitution by asparagine probably destabilizes the G-domain in the GDP-inactive state, which may explain the decrease in nucleotide association. In contrast, K5 points to the solvent exterior in the GTP-state and is not located within the interacting interface contacting GAPs and effectors (Supp. Fig. S1). Therefore, it is unlikely that a K5N mutation will affect the GAP or effector interaction, which is in good agreement with the *in vitro* biochemical data (Table 1).

T58 is almost completely buried in the GTP-bound state (Supp. Table S3), and is surrounded by several critical residues, including Q61, G60, D57 and Y71 (Supp. Fig. S7B). The hydroxyl group of T58 forms an intramolecular hydrogen bond with the oxygen of V8. Insertion of a methyl group by the mutation to isoleucine may shift the overall structural integrity. The residue E153 (replaced by the homologous residue D153 in KRAS; Supp. Fig. S6) is an integral element of the intermolecular interaction network involving N26, R149, Y157 and the nucleotide contacting residues F28 and K147 (Supp. Fig. S7C). One might think of that an alteration of E153 to valine, may lead to disruption of this interacting network and consequently result in increased RAS activation, a scenario which has recently been suggested for the $KRAS^{D153V}$ (Carta et al., 2006; Schubbert et al., 2007). In our comprehensive study, however, there is no indication that a substitution of E153 by valine

changes biochemical functions of RAS that could be interrogated by the panel of *in vitro* functional assays used. Similarly, Fig. 5 and Supp. Fig. S4 showed that $KRAS^{D153V}$ expressing cells did not exhibit any difference regarding pERK and pAKT levels as compared to $KRAS^{wt}$. But unlike the other mutants, we observed an increase in MEK phosphorylation only in the case of D153V mutant. Whether this is due to a slightly higher GTP-bound level of this mutant remains to be investigated.

Class B mutants ($KRAS^{V14I}$): the only one member of that group so far, $KRAS^{V14I}$ is characterised by an strong increase of both, intrinsic and GEF-catalysed nucleotide exchange, leading to an increased level of the activated state (Fig. 2).V14 is completely buried in both, the GDP- and GTP-bound states of RAS (Supp. Table S3; Supp. Fig. S7D) and its alteration most likely influences the overall structural integrity of such a globular protein. Substitution of V14 by the larger isoleucine in the G1 motif (P-loop) likely generates a sterical clash with the surrounding residues (Supp. Fig. S7D), thereby changing the overall structure of the phosphate binding loop.

Class C mutants ($KRAS^{Q22R}$): the characteristics of class C mutants represented by $KRAS^{Q22R}$ is an impaired GAP-stimulated GTP hydrolysis, with unaffected intrinsic functions and a virtually functional effector interaction (Fig 6). Q22 is positioned at the edge of the interaction surface of RAS and in interaction with the sidechains of F28 and K147 (see below, in Class D), as well as R149. Replacement of Q22 by an arginine most likely lead to a surface exposed guanidium group of the arginine that interferes with the GAP binding (Supp. Fig. S7C) but does not interfere with effector binding (Fig. 6).

Class D mutants ($KRAS^{Q22E}$, $KRAS^{F156L}$): Class D members exhibit an increase in intrinsic and GEF catalyzed nucleotide exchange, in combination with an impaired GAP-stimulated GTP hydrolysis, but functional in interaction with effectors. Q22 and F156 are not directly involved in coordination of the active center. Q22 contacts two amino acids, F28 and K147, which are critical for nucleotide binding (Supp. Fig. S7C). The former one, when mutated to leucine, was shown to transform PC12 cells and cause a dramatic increase in nucleotide dissociation, generating the so-called 'fast cycling' RAS mutant protein (Reinstein. et al., 1991). F156 is completely buried in both, the GDP- and GTP-bound states of RAS (Supp. Fig. S7E) and its alteration most likely influences the overall structural integrity.

Mutation of the completely buried F156 to the smaller leucine appears to create a relatively large cavity that obviously might have two significant consequences, changes in the dynamics of protein interior that impairs the nucleotide exchange and alterations on the protein surface that affects the interaction with GAP and effectors. Substitutions of Q22 seem to obey different scenario. While the larger side chain of arginine in $KRAS^{Q22R}$ can just point to the solvent without affecting the integrity of structure, the glutamate carboxyl of $KRAS^{Q22E}$

may disturb the networks of intramolecular interactions and alters thus the dynamics of RAS similarly to the $KRAS^{V14I}$ and $KRAS^{F156L}$ mutants.

Class E mutants ($KRAS^{P34L}$, $KRAS^{P34R}$, $KRAS^{G60R}$): these mutants are characterized by a defective GAP sensitivity and a strongly reduced interaction with effectors. P34 is located at the center of the interacting interface. Interestingly, although being an integral part of the switch I region it does not change its solvent exposure between the GDP- and GTP- bound states. Therefore, its substitution to leucine or arginine directly impairs the interaction of RAS with these two classes of binding partners through electrostatic or steric clashes (Supp. Fig. S7F). Whether P34 mutations also lead to alterations in the switch I conformation remains to be clarified. The mutation of KRAS G60 to arginine leads to an overall impairment of almost all biochemical and functional properties. G60 has a high degree of conformational flexibility within the RAS structure. G60 is solvent exposed in the GDP-bound state and shifts by 4.8 Å to form a hydrogen bond with the γ-phosphate of GTP upon RAS activation (Supp. Fig. S7G).

References

Ahmadian, M.R., Zor, T., Vogt, D., Kabsch, W., Selinger, Z., Wittinghofer, A., Scheffzek, K. (1999) *Proc. Natl. Acad. Sci.* USA **96**, 7065-7070.

Boriack-Sjodin, P.A., Margarit, S.M., Bar-Sagi, D., Kuriyan, J. (1998) *Nature* **394**, 337-343.

Buhrman, G.K., de Serrano, V., Mattos, C. (2003) *Structure* **11**, 747-751.

Buhrman, G., Wink, G., Mattos, C. (2007) *Structure* **15**, 1618-1629.

Bunney, T.D., Harris, R., Gandarillas, N.L., Josephs, M.B., Roe, S.M., Sorli, S.C., Paterson, H.F., Rodrigues-Lima, F., Esposito, D., Ponting, C.P., Gieschik, P., Pearl, L.H., Driscoll, P.C., Katan, M. (2006) *Mol. Cell* **21**, 495-507.

Carta, C., Pantaleoni, F., Bocchinfuso, G., Stella, L., Vasta, I., Sarkozy, A., Digilio, C., Palleschi, A., Pizzuti, A., Grammatico, P., Zampino, G., Dallapiccola, B., Gelb, BD., Tartaglia M (2006) *Am. J. Hum. Genet.* **79**, 129-135.

Cirstea, I.C., Kutsche, K., Dvorsky, R., Gremer, L., Carta, C., Horn, D., Roberts, A.E., Lepri, F., Merbitz-Zahradnik, T., König, R., Kratz, C.P., Pantaleoni, F., Dentici, M.L., Joshi, V.A., Kucherlapati, R.S., Mazzanti, L., Mundlos, S., Patton, M.A., Silengo, M.C., Rossi, C., Zampino, G., Digilio, C., Stuppia, L., Seemanova, E., Pennacchio, L.A., Gelb, B.D,, Dallapiccola, B., Wittinghofer, A., Ahmadian, M.R., Tartaglia, M., Zenker, M. (2010) *Nat. Genet*. **42,** 27-29.

Denayer, E., Parret, A., Chmara, M., Schubbert. S., Vogels. A., Devriendt, K., Frijns, J.P., Rybin, V., de Ravel, T.J., Shannon, K., Cools, J., Scheffzek, K., Legius, E. (2008) *Hum. Mutat.* **29**, 232-239.

Ford, B, Hornak, V, Kleinman, H, Nassar, N. (2006) *Structure* **14**, 427-436.

Ford, B, Skowronek, K, Boykevisch, S, Bar-Sagi, D, Nassar, N. (2005) *J. Biol. Chem.* **280**, 25697-25705.

Franken, S.M., Scheidig, A.J., Krengel, U., Rensland, H., Lautwein, A., Geyer, M., Scheffzek, K., Goody, R.S., Kalbitzer, H.R., Pai, E.F. (1993) *Biochem.* **32**, 8411-8420.

Hall, B.E., Bar-Sagi, D., Nassar, N. (2002) *Proc. Natl. Acad. Sci.* USA **99**, 12138-12142.

Huang, L., Hofer, F., Martin, G.S., Kim, S.H. (1998) *Nat. Struct. Biol.* **5**, 422-426.

Ito, Y., Yamasaki, K., Iwahara, J., Terada, T., Kamiya, A., Shirouzu, M., Muto, Y., Kawai, G., Yokoyama, S., Laue, E.D., Walchli, M., Shibata, T., Nishimura, S., Miyazawa, T. (1997) *Biochem.* **36**, 9109-9119.

Kigawa, T., Yamaguchi-Nunokawa, E., Kodama, K., Matsuda, T., Yabuki, T., Matsuda, N., Ishitani, R., Nureki, O., Yokoyama, S. (2001) *J. Struct. Funct. Genom.* **2**, 29-35.

Klink, B.U., Goody, R.S., Scheidig, A.J. (2006) *Biophys. J.* **91**, 981-992.
Kraulis, P.J., Domaille, P.J., Campbell-Burk, S.L., Van Aken, T., Laue, E.D. (1994) *Biochem.* **33**, 3515-3531.
Krengel, U. (1991) Ph. D. Thesis, Heidelberg
Krengel, U., Schlichting, I., Scherer, A., Schumann, R., Frech, M., John, J., Kabsch, W., Pai, E.F., Wittinghofer, A. (1990) *Cell* **62**, 539-548.
Margarit, S.M., Sondermann, H., Hall, B.E., Nagar, B., Hoelz, A., Pirruccello, M., Bar-Sagi, D., Kuriyan, J. (2003) *Cell* **112**, 685-695.
Milburn, M.V., Tong, L., deVos, A.M., Brunger, A., Yamaizumi, Z., Nishimura, S., Kim, S.H. (1990) *Science* **247**, 939-945.
Pacold, M.E., Suire, S., Perisic, O., Lara-Gonzalez, S., Davis, C.T., Walker, E.H., Hawkins, P.T., Stephens, L., Eccleston, J.F., Williams, R.L. (2000) *Cell* **103**, 931-943.
Pai, E.F., Krengel, U., Petsko, G.A., Goody, R.S., Kabsch, W., Wittinghofer, A. (1990) *EMBO J.* **9**, 2351-2359.
Reinstein, J., Schlichting, I., Frech, M., Goody, R.S., Wittinghofer, A. (1991) *J. Biol. Chem.* **266**, 17700-17706.
Scheffzek, K., Ahmadian, M.R., Kabsch, W., Wiesmuller, L., Lautwein, A., Schmitz, F., Wittinghofer, A. (1997) *Science* **277**, 333-338.
Scheffzek, K., Grunewald, P., Wohlgemuth, S., Kabsch, W., Tu, H., Wigler, M., Wittinghofer, A., Herrmann, C. (2001) *Structure* **9**, 1043-1050.
Scheidig, A.J., Burmester, C., Goody, R.S. (1999) *Structure* **7**, 1311-1324.
Scheidig, A.J., Franken, S.M., Corrie, J.E., Reid, G.P., Wittinghofer, A., Pai, E.F., Goody, R.S. (1995) *J. Mol. Biol.* **253**, 132-150.
Scheidig, A.J., Sanchez-Llorente, A., Lautwein, A., Pai, E.F., Corrie, J.E.T., Reid, G.P., Wittinghofer, A., Goody, R.S. (1994) *Acta Crystallogr.* **D50**, 512-520.
Schubbert, S., Bollag, G., Lyubynska, N., Nguyen, H., Kratz, C.P., Zenker, M., Niemeyer, C.M., Molven, A., Shannon, K. (2007) *Mol. Cell. Biol.* **27**, 7765-7770.
Schweins, T., Scheffzek, K., Assheuer, R., Wittinghofer, A. (1997) *J. Mol. Biol.* **266**, 847-856.
Sondermann, H., Soisson, S.M., Boykevisch, S., Yang, S.S., Bar-Sagi, D., Kuriyan, J. (2004) *Cell* **19**, 393-405.
Spoerner, M., Herrmann, C., Vetter, I.R., Kalbitzer, H.R., Wittinghofer, A. (2001) *Proc. Natl. Acad. Sci.* USA **98**, 4944-4949.
Stieglitz, B., Bee, C., Schwarz, D., Yildiz, O., Moshnikova, A., Khokhlatchev, A., Herrmann, C. (2008) EMBO J. **27**, 1995-2005.
Tanaka, T., Williams, R.L., Rabbitts, T.H. (2007) EMBO J. **26**, 3250-3250.
Tong, L.A., de Vos, A.M., Milburn, M.V., Kim, S.H. (1991) *J. Mol. Biol.* **217**, 503-516.

Table 1 Summary of biochemical properties of the RAS proteins grouped into five classes

Classes	RAS mutant	mant-GppNHp association	Intrinsic mantGDP dissociation	GEF-catalyzed mantGDP dissociation	Intrinsic GTPase	GAP-stimulated GTPase	RAF-RBD binding
controls	wt	1.3[a]	0.00003[a]	0.09[a]	0.0093[a]	9.3[a]	0.22[b]
	G12V	≈	≈	≈	↓	⬇	↓
	F28L	↑	↑	↑	≈	↓	⬇
A	K5N	⇩	≈	≈	≈	≈	≈
	T58I	≈	↑	≈	≈	≈	↓
	E153V	↓	≈	≈	≈	≈	↓
B	V14I	↓	⇧	⇧	≈	≈	↓
C	Q22R	↓	≈	≈	≈	⇩	≈
D	Q22E	↓	⇧	⇧	≈	⇩	↓
	F156L	↓	⬆	⇧	≈	⇩	⇩
E	P34L	≈	≈	≈	≈	⬇	⬇
	P34R	≈	≈	≈	≈	⬇	⬇
	G60R	↓	≈	⬇	↓	⬇	⬇

Based on our biochemical data, RAS mutants are grouped into different functional classes: (A) no major changes; (B) increase in intrinsic and catalyzed nucleotide exchange; (C) decrease in GAP-stimulated GTPase; (D) increase in intrinsic and catalyzed nucleotide exchange and decreased in GAP-stimulated GTPase; (E) defective interaction with GAPs and effectors and also with GEFs in the case of RAS^{G60R}. RAS^{wt}, RAS^{G12V} and RAS^{F28L} were included as controls. Black arrows outlines effects that favor increased signaling, grey arrows those impaired signaling, such as lower affinity of effectors. ≈ ≤ 2-fold, ↓ or ↑ = 3-15-fold, ⇩ or ⇧ = 15-40-fold, ⬇ or ⬆ >40-fold relative to RAS^{wt} values. Relative values are shown in Table S4. [a] observed rate constants (k_{obs}) in sec^{-1}; [b] dissociations constants (K_d) in µM.

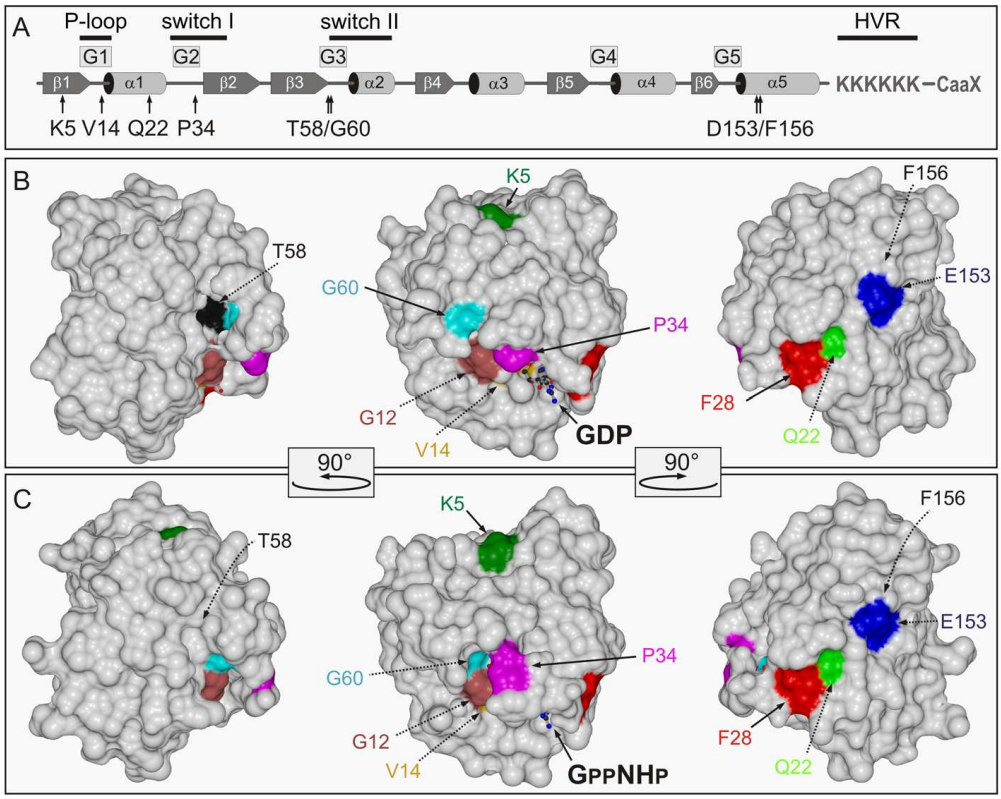

119x96mm (300 x 300 DPI)

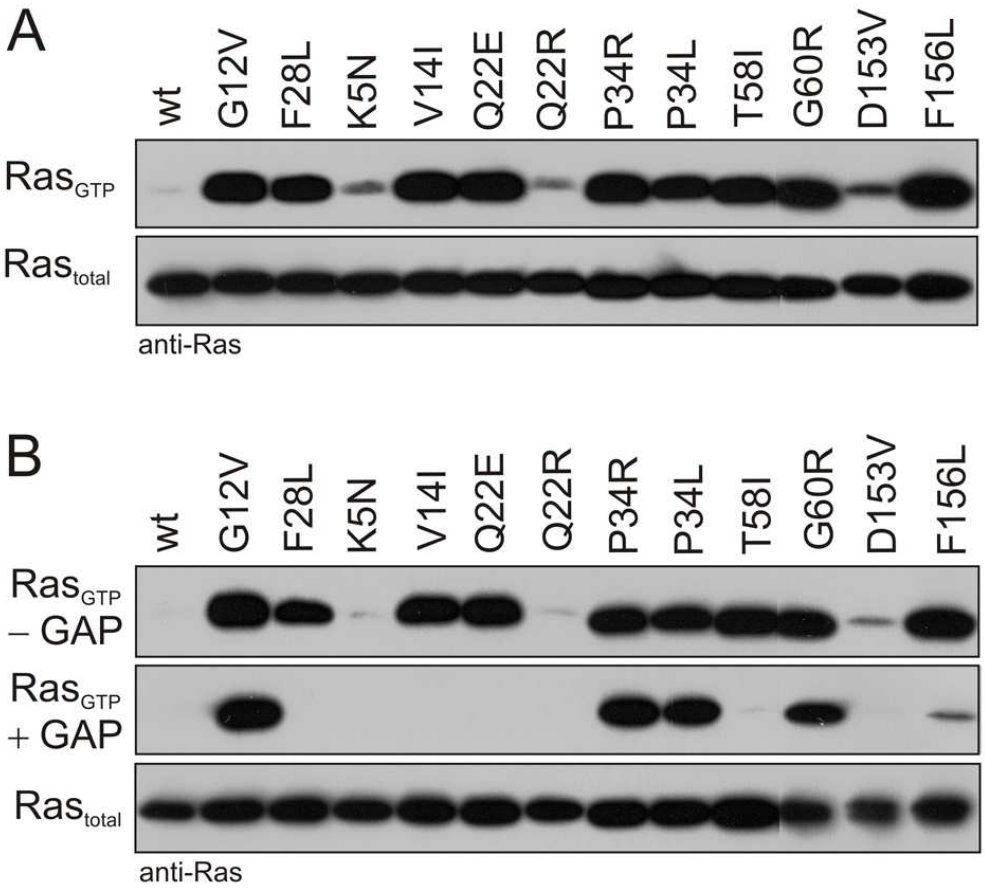

80x71mm (300 x 300 DPI)

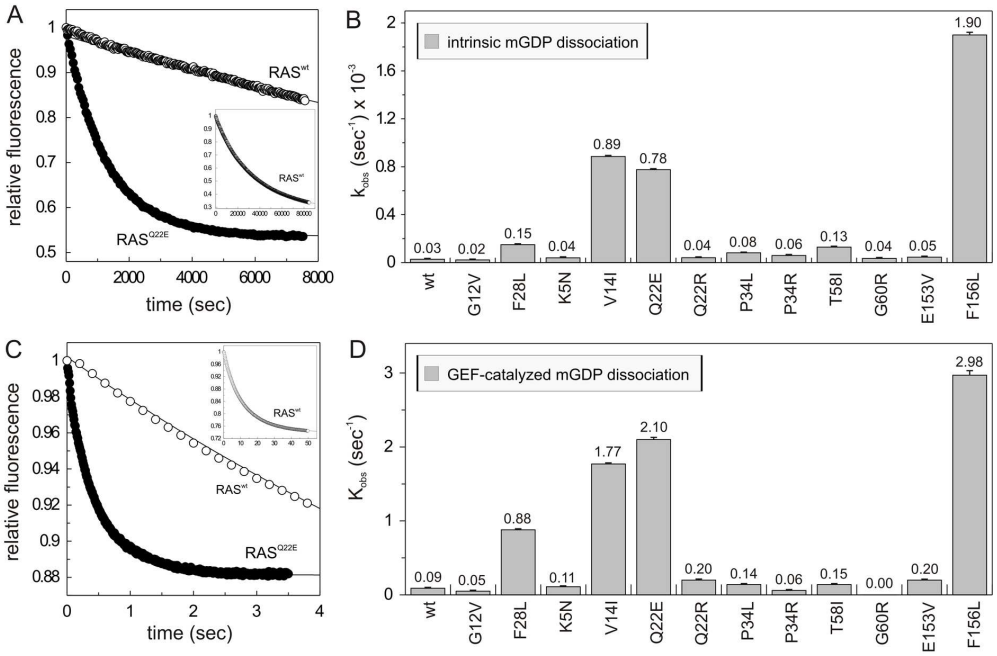

160x105mm (300 x 300 DPI)

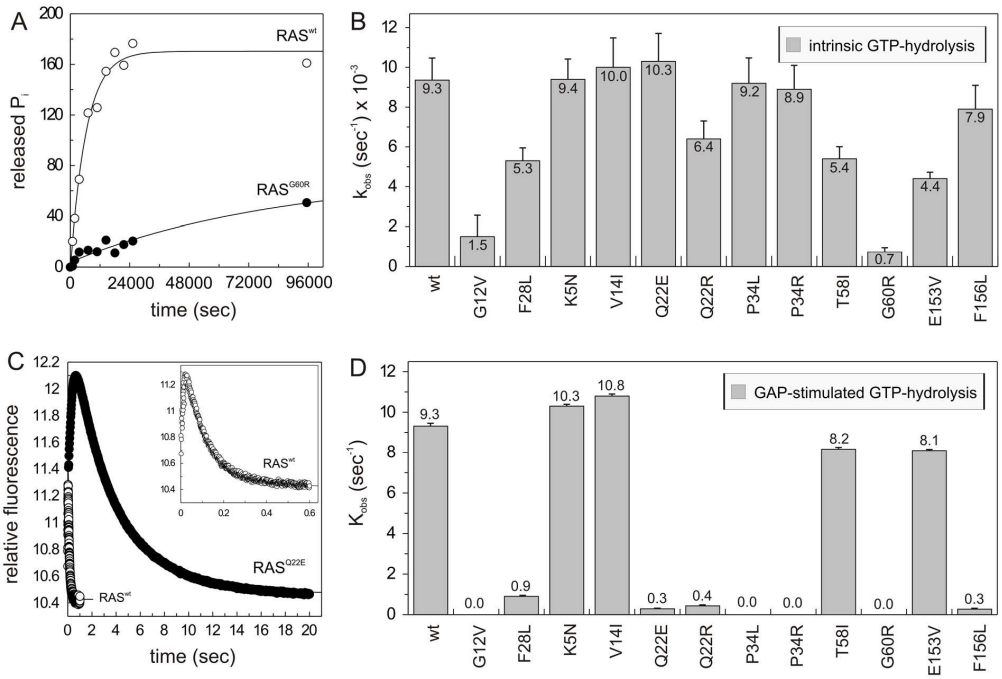

160x108mm (300 x 300 DPI)

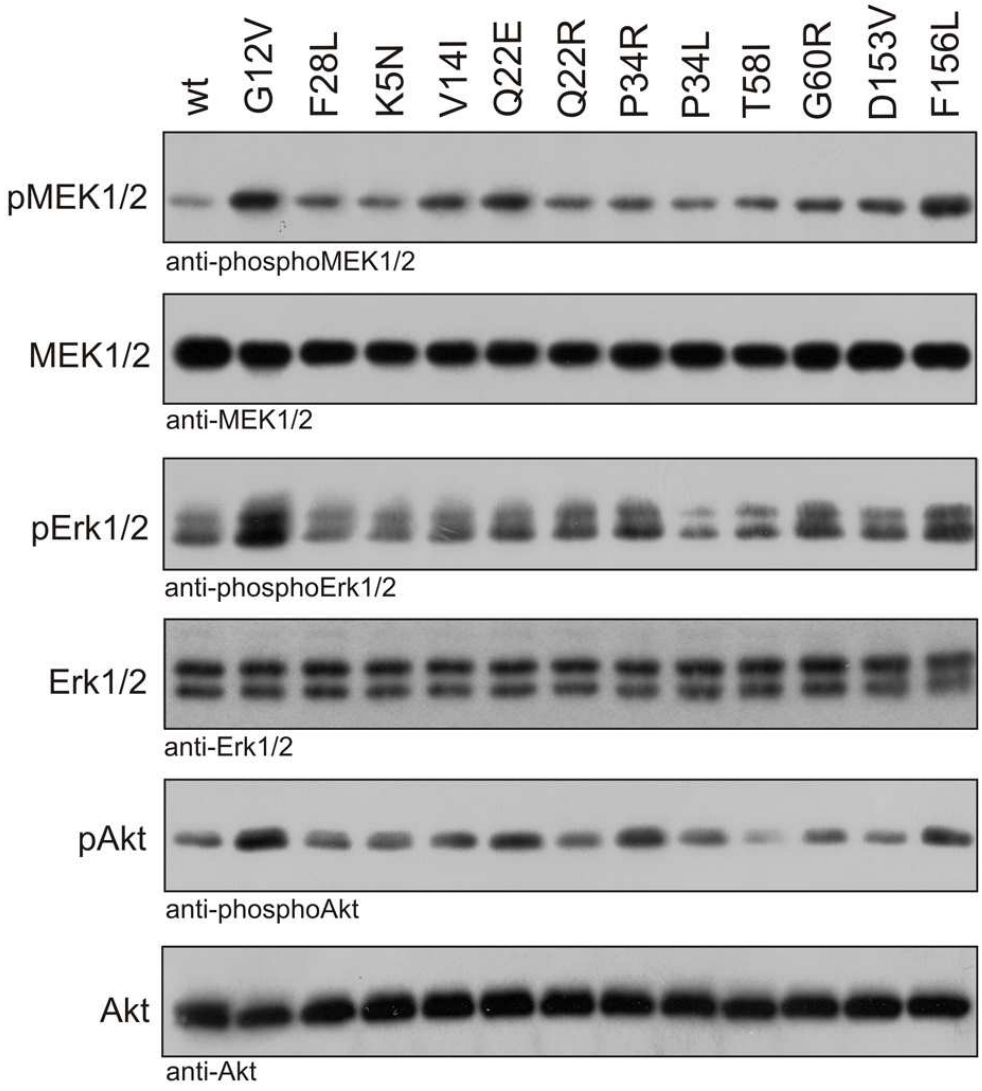

80x87mm (300 x 300 DPI)

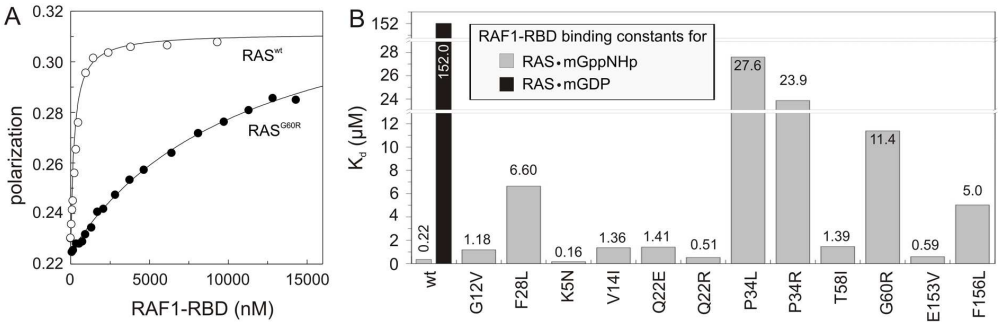

160x51mm (300 x 300 DPI)